PHILOSOPHICAL TRANSACTIONS A

royalsocietypublishing.org/journal/rsta

Research

Cite this article: Zubizarreta Casalengua E, Laussy FP, del Valle E.. 2024 Two photons everywhere. *Phil. Trans. R. Soc. A* **382**: 20230315.
https://doi.org/10.1098/rsta.2023.0315

Received: 21 February 2024
Accepted: 14 July 2024

One contribution of 15 to a theme issue 'Celebrating the 15th anniversary of the Royal Society Newton International Fellowship'.

Subject Areas:
atomic and molecular physics, quantum physics, spectroscopy, optics

Keywords:
squeezing, antibunching, bunching, correlations, interferences

Author for correspondence:
E. del Valle
e-mail: elena.delvalle.reboul@gmail.com

Two photons everywhere

E. Zubizarreta Casalengua[1], F. P. Laussy[3] and E. del Valle[4,2]

[1]Walter Schottky Institute, School of Computation, Information and Technology and MCQST, and [2]Institute for Advanced Study, Technische Universität München, Garching 85748, Germany
[3]Instituto de Ciencia de Materiales de Madrid ICMM-CSIC, Madrid 28049, Spain
[4]Departamento de Física Teórica de la Materia Condensada e IFIMAC, Universidad Autónoma de Madrid, Madrid 28049, Spain

EZC, 0000-0003-4967-595X; FPL, 0000-0002-1070-7128; E.dV, 0000-0002-0221-282X

We discuss two-photon physics, taking for illustration the particular but topical case of resonance fluorescence. We show that the basic concepts of interferences and correlations provide at the two-photon level an independent and drastically different picture than at the one-photon level, with landscapes of correlations that reveal various processes by spanning over all the possible frequencies at which the system can emit. Such landscapes typically present lines of photon bunching and circles of antibunching. The theoretical edifice to account for these features rests on two pillars: (i) a theory of frequency-resolved photon correlations and (ii) admixing classical and quantum fields. While experimental efforts have been to date concentrated on correlations between spectral peaks, strong correlations exist between photons emitted away from the peaks, which are accessible only through multi-photon observables. These could be exploited for both fundamental understanding of quantum-optical processes as well as applications by harnessing these unsuspected resources.

This article is part of the theme issue 'Celebrating the 15th anniversary of the Royal Society Newton International Fellowship'.

1. Introduction

Quantum mechanics is notorious for its quantized spectral lines. This is how the theory was born and

THE ROYAL SOCIETY PUBLISHING

royalsocietypublishing.org/journal/rsta Phil. Trans. R. Soc. A 382: 20230315

the fact after which it is named, following Bohr [1]'s quantization of angular momentum of the electron orbitals in the hydrogen atom. This provided Rydberg's constant as a product of fundamental constants and explained the lines as transitions between energy levels (figure 1*a*). At about the same time, a much less resounding finding was recorded in a bulletin of the Lowell Observatory: a nebula in the Pleiades was observed to have a completely continuous spectrum of emission [2]. There are many ways to produce a continuous spectrum, from unbound charges to, as was the case here, scattering from a broad spectrum (the light from the star Merope). Systematic and careful observations revealed that emission nebulae (in particular planetary nebulae), which do not reflect but emit light directly, also feature a continuous spectrum in addition to the spectral lines of what was by then well-established quantum theory [3]. One part—the Balmer continuum—could be explained with the known mechanisms from reflection nebulae, but on the other side of the Balmer limit, sitting with the quantized spectral lines in the visible spectrum, lay a continuum spectrum which was of unknown origin [4]. This was simultaneously and independently resolved in 1950, from both sides of the iron curtain [5,6], as a fitting companion to Bohr's model of quantum jumps in the form of a two-photon emission from the metastable $2s_{1/2}$ shell of the hydrogen atom down to the ground state $1s_{1/2}$ (figure 1*a*). Would the atom be excited in the $2p$ level, it would undergo a normal, 'Bohrian' transition back to the ground state, but the $2s$–$1s$ is dipole forbidden so it has to go through the next (quadrupole) order, which is however very weak, and, in ambient conditions, is knocked-off by collision back into a radiative state. In the extremely rarefied cosmic conditions, however, there is plenty of space as well as enough time to have isolated hydrogen atoms left stuck in great quantity in their $2s$ state. For those, the next best route back to $1s$ is the 'Doppelemission' (double-emission or two-photon emission) theorized by Göppert Mayer [7] and first applied to hydrogen by Breit and Teller [8]. Although a higher order process, it is not dipole forbidden and finds in outer space the ideal quiet laboratory conditions making possible its direct observation, indeed giving it the name of 'visual continuum'. The Earth-based laboratory is less auspicious for a direct (visual) observation of two-photon emission [9], but the process nevertheless opened the multi-photon page of atomic physics [10]. Such two-photon transitions have, among other things, been generalized to link any (n, l, m) states of the atom [11] and can be stimulated with a laser [12]. In the solid state, the opposite regime of the interstellar one can be realized with high populations in small volumes, e.g. in semiconductors, where delocalized electrons in the crystal under high laser excitation can jump the bandgap in sufficient amount to produce a measurable and even controllable two-photon continuous spectrum [13]. Another solid-state approach is to inflate the light-matter coupling by focusing light onto the emitter, to make higher order processes 'less smaller' and thus lift their 'forbidden' character, possibly making them even comparable to first-order processes [14].

Here, we present a quantum optical alternative to the quantum electrodynamics description. The latter typically relies on a perturbative treatment of the two-photon processes of a complex system: the hydrogen atom in its simplest case, up to an interstellar ionized gas bathed in the radiation of other astronomical objects. Instead, we consider the exact treatment of a simple system, namely, resonance fluorescence, i.e. the photon emission (fluorescence) of a two-level system driven at the same energy as it is excited (resonance). This will allow us to focus on the two-photon physics itself, instead of interesting but secondary problems specific to hydrogen or to the thermodynamics of nebulae. While we invoke a variety of our results collected over the last decade, we try to keep the discussion self-contained with no need of prior familiarity with our earlier works on, mainly, frequency-resolved multi-photon correlations [15] or multi-photon interferences of quantum fields [16]. We furthermore connect these two aspects to provide a new and fairly comprehensive picture of the phenomenology of two-photon emission from resonance fluorescence, explaining features hitherto only observed. Section 2 introduces the textbook problem of resonance fluorescence but revisited with the 'sensor formalism' [15], which is an alternative way to compute spectra that will allow us, in §3, to provide a first departure from conventional treatments, by introducing our concept of

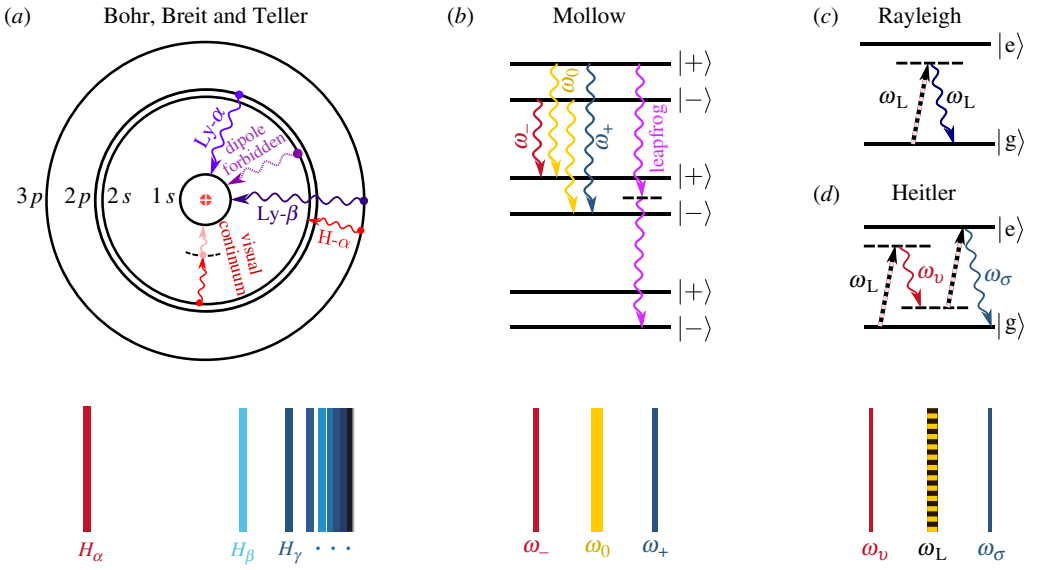

Figure 1. (*a*) Old quantum mechanics: transitions between quantized orbitals of the electron lead to a quantized spectrum. Transitions to $n = 2$ form the visible (Balmer) series. The $2 \longrightarrow 1$ (Lyman) is in the ultraviolet. The $2s \longrightarrow 1s$ is, however, dipole forbidden, but it can occur with a continuum of two-photon emission, which falls again in the visible range. (*b*) Transitions between dressed states $|\pm\rangle$ lead to a triplet (Mollow) spectrum. A two-photon, so-called *leapfrog*, transition can also occur that jumps over an intermediate state. However weak is this transition, it can be revealed by two-photon correlations. (*c*) In the low-driving limit, detuning makes the same physics take another turn, with the triplet now formed by the Rayleigh scattering as the central peak and (*d*) breaking the leapfrog over one real-state transition but keeping the other one virtual, accounting for the two side peaks. This results in a rich two-photon physics beyond the side peaks, not visible in photoluminescence but revealed in the two-photon correlation spectrum.

frequency-resolved correlations, which will put the two-photon observables on the same footing as the one-photon ones, and explain the reason for our title of 'two photons everywhere'. In §4, we introduce the other pillar of our edifice: interferences of quantum fields, as underpinning their statistical properties [16]. The basic idea, that holds with quantum states, is applied to a dynamical system in §5, which, in spirit, is resonance fluorescence itself, but we show that the two-photon observables are actually captured by the simpler case of a squeezed cavity, allowing us to identify what is specific to quantum states admixtures of Gaussian states (squeezing and coherent states) and what is to the 'more quantum' two-level system, to which we return in §6 with a focus on detuning. We provide a surprisingly compact expression for two-photon correlations in this case, that is exact to leading order in the driving and captures its main phenomenology. In §7, we show how our approach gives way to countless variations, even if remaining at the level of resonance fluorescence, although this could and should be extended to all possible quantum emitters. Specifically, we consider entanglement and other quantum resources such as two-mode squeezing, which we merely exhibit but that could be similarly explained and exploited. Our approach could also usefully revisit closely related problems such as two-photon absorption [17], two-photon resonance fluorescence [18] or two-photon gain [19].

2. Resonance fluorescence

Resonance fluorescence is the simplest problem of quantum optics, yet a still actively investigated one. Its Hamiltonian in the rotating frame of the laser is (with $\hbar = 1$)

$$H_\sigma \equiv \Delta_\sigma \sigma^\dagger \sigma + \Omega_\sigma(\sigma^\dagger + \sigma), \tag{2.1}$$

where σ is the annihilation operator of a two-level system driven coherently by a laser with amplitude $\Omega_\sigma \in \mathbb{R}$, and Δ_σ is the detuning from the laser frequency ω_L, which we shall take as the reference, i.e. $\omega_L = 0$. This problem provides a rich quantum-optical playground, from essentially two regimes of excitation: at low-driving (so-called Heitler regime [20]), the spectrum is dominated by the Rayleigh-scattered light of the laser, while at high-driving (so-called Mollow regime [21]), there is a splitting of the spectral shape into a triplet (figure 1*b*). While these two regimes are very different in character, we can find a first unifying theme through large detuning. When the laser drives the system far from its resonance frequency (although still referring to 'resonance fluorescence'), the spectral response remains a symmetric triplet. This is shown at the top of figure 2 for: (i) the Mollow triplet at resonance, (ii) the detuned Mollow triplet with an increasingly bright coherent peak sitting on top of a dim fluorescent one, and (iii) the detuned (Heitler regime of) resonance fluorescence with vanishing fluorescent contributions. The driving Ω_σ has been chosen so that the spectral position of the side peaks is the same in units of the Mollow splitting $\Omega_+ \approx \sqrt{\Delta_\sigma^2 + 4\Omega_\sigma^2}$ (at large enough detunings). The frequency ω is normalized to this splitting, i.e. $\varpi \equiv (\omega - \omega_L)/\Omega_+$. The central peak is either (figure 2*a*) a fluorescent (broad) peak, (figure 2*c*) the Rayleigh-scattered coherent peak (intense and narrow central peak, note that the side peaks are magnified by a factor 800) or (figure 2*b*) an admixture of a fluorescent and coherent peaks.

One can conveniently derive such results with our sensor formalism [15], which is an alternative to formal results that rely on mathematical structures of the problem—such as the quantum regression theorem or the Wiener–Khinchin theorem—to obtain instead observables from a physical modelling of what is being measured. This was developed to extend the physical spectrum of Eberly and Wódkiewicz [22] to N-photon observables, which instead of computing awkward multi-time, normally ordered integrals, simply attaches to the system 'sensors' (two of them for two-photon correlations, N sensors in general) and computes correlations directly from their usual quantum averages. Technically, this requires to 'plug' to the Hamiltonian of the system (in our case, equation (2.1)), the sensors, themselves most simply described as two-level systems ς_i whose frequencies ω_i define which frequencies are being 'measured'. The name 'sensor' was chosen as opposed to 'detector' since correlations are obtained in the limit $\epsilon \to 0$ of their vanishing coupling to the system, thereby not affecting its dynamics. This restricts their use to correlations as opposed to signal. Alternatively, one can also use the 'cascading systems' [23,24], which was shown in [25] to be equivalent to the sensor method and to conveniently substitute it in cases where the signal is needed, e.g. to perform frequency-resolved Monte Carlo simulations [25]. For resonance fluorescence, the augmented Hamiltonian thus reads:

$$H_{\sigma;\varsigma} \equiv H_\sigma + \Delta_1 \varsigma_1^\dagger \varsigma_1 + \Delta_2 \varsigma_2^\dagger \varsigma_2 + \epsilon \sum_{i=1,2} (\sigma^\dagger \varsigma_i + \varsigma_i^\dagger \sigma) \,. \tag{2.2}$$

In the rotating frame of the laser, the frequencies $\Delta_i \equiv \omega_i - \omega_L$ are simply ω_i since $\omega_L = 0$. As a quantum-optical problem, one should include dissipation, which can be provided by a master equation in the Lindblad form, so that the dynamics for the full density matrix ρ—of the system itself as well as its sensors—is governed by the equation

$$\partial_t \rho = -i[H_\sigma, \rho] + \frac{\gamma_\sigma}{2} \mathcal{L}_\sigma \rho + \sum_{j=1,2} \frac{\gamma_j}{2} \mathcal{L}_{\varsigma j} \rho, \tag{2.3}$$

where the Lindblad terms are of the form $\mathcal{L}_c \rho \equiv 2c\rho c^\dagger - c^\dagger c\rho - \rho c^\dagger c$ for any operator c. Importantly, in addition to the decay rate γ_σ of the two-level system, we also bring the decay rate γ_i of the ith sensor, that describes its frequency bandwidth. For two-photon observables (and higher N), such a parameter is mandatory for a physical description of the system, unlike one-photon observables like the power spectrum, which can be well described for a vanishing linewidth of their detector (recovering the Wiener–Khinchin result). In the following, we shall assume the

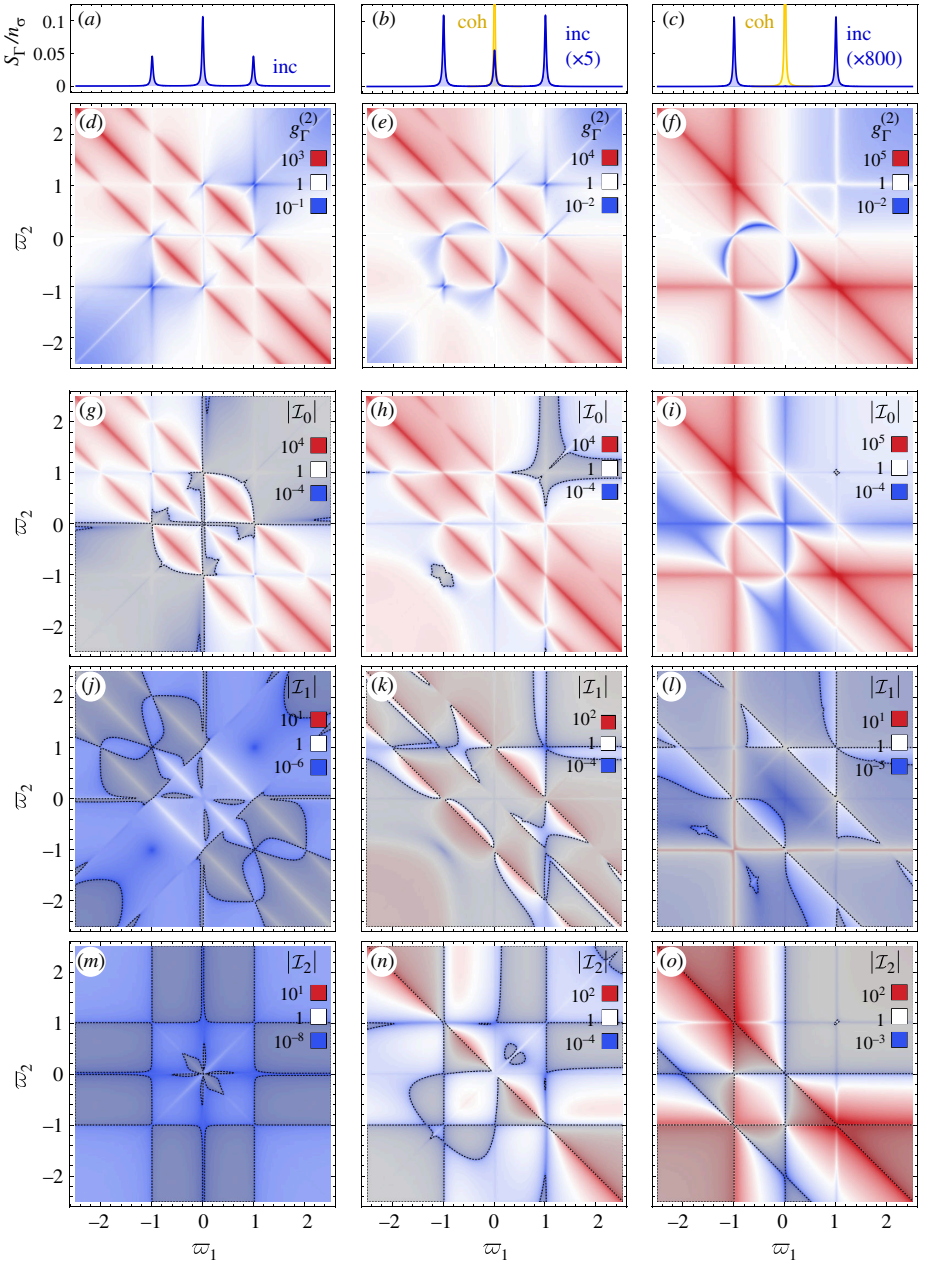

Figure 2. The two-photon physics of resonance fluorescence. Top row: photoluminescence spectra for (*a*) the Mollow triplet at resonance, (*b*) the detuned Mollow triplet and (*c*) the detuned Heitler triplet. The coherent (scattered) light is shown in yellow. Second row: two-photon correlation spectra $g^{(2)}_\Gamma(\varpi_1, \varpi_2)$ for the corresponding spectra, with bunching in red, no-correlation in white and antibunching or no-coincidence emission in blue. Two sets of features dominate the landscape: straight lines of bunching (red) and circles of antibunching (blue). Lines result from multi-photon transitions that involve virtual photons—'leapfrog processes'—while circles result from self-homodyning destructive interferences. Three bottom rows: covariance $\mathcal{I}_0$ (third row), anomalous two-photon moments $\mathcal{I}_1$ (fourth) and squeezing $\mathcal{I}_2$ (bottom) which sum together with 1 to the two-photon spectrum according to equation (4.14). The right column, that is squeezing dominated, is well approximated by equations (6.8). Shaded regions refer to negative quantities. Parameters: $\gamma_\sigma = 1$ (setting the unit) and $\Gamma = 2$ everywhere, while $(\Delta_\sigma, \Omega_\sigma) = (a)\ (0, 40.05)$, $(b)\ (60, 26.53)$ and $(c)\ (80, 2)$.

royalsocietypublishing.org/journal/rsta Phil. Trans. R. Soc. A 382: 20230315

same frequency resolution for both sensors, i.e. $\gamma_{1,2} = \Gamma$, which we shall refer to as the 'filter width' as this also corresponds to placing an interference filter before an ideal detector. The sensor method allows us to obtain the luminescence spectrum $S_\Gamma(\omega) = \frac{\Gamma}{2\pi\epsilon^2}\langle\zeta^\dagger\zeta\rangle(\omega)$ (no index needed since a single sensor is enough) as the population of the sensor ζ placed at the frequency ω, which is a mere parameter in equation (2.2) as opposed to a physical observable and thus an operator, which would complicate very much the treatment. In particular, note that we need not invoke any quantum-regression theorem, Fourier transform, etc. For resonance fluorescence, the spectral shape has a simple, characteristic structure:

$$S_\Gamma(\omega) = |\langle\sigma\rangle|^2 \mathscr{L}_\Gamma(\omega) + \big(\langle\sigma^\dagger\sigma\rangle - |\langle\sigma\rangle|^2\big).\mathscr{M}_\Gamma(\omega) \tag{2.4}$$

where

$$\langle\sigma\rangle = \frac{2\Omega_\sigma(2\Delta_\sigma + i\gamma_\sigma)}{\gamma_\sigma^2 + 4\Delta_\sigma^2 + 8\Omega_\sigma^2} \quad \text{and} \quad \langle\sigma^\dagger\sigma\rangle = \frac{4\Omega_\sigma^2}{\gamma_\sigma^2 + 4\Delta_\sigma^2 + 8\Omega_\sigma^2} \tag{2.5}$$

are the coherently scattered field $\langle\sigma\rangle$ (with intensity the modulus square of this) and the total population $\langle\sigma^\dagger\sigma\rangle$, including the coherent part, so the incoherent part alone is $\langle\sigma^\dagger\sigma\rangle - |\langle\sigma\rangle|^2 = 32\Omega_\sigma^4/(\gamma_\sigma^2 + 4\Delta_\sigma^2 + 8\Omega_\sigma^2)^2$ (this happens to be $2\langle\sigma^\dagger\sigma\rangle^2$). Note that these are not Γ dependent. They weight, respectively, a central Lorentzian peak $\mathscr{L}_\Gamma(\omega) \equiv \frac{1}{\pi}\frac{\Gamma/2}{(\Gamma/2)^2 + \omega^2}$ and a symmetric triplet (both normalized), whose expression is a bit more involved:

$$\mathscr{M}_\Gamma(\omega) \equiv \tag{2.6}$$

$$\frac{2}{\pi}\frac{(\gamma_{12}^2 + 4\omega^2)(\gamma_{11}^2\gamma_{12} + 4\gamma_{12}\Delta_\sigma^2 + 4\gamma_{10}\omega^2) + 8\Omega_\sigma^2(\gamma_{11}\gamma_{12}\gamma_{35} + 4\gamma_{12}\Delta_\sigma^2 - 4\gamma_{1\bar{5}}\omega^2) + 128\Omega_\sigma^4\gamma_{11}}{(\gamma_{12}^2 + 4\omega^2)\big[(\gamma_{11}^2 + 4\Delta_\sigma^2)^2 + 8(\gamma_{11}^2 - 4\Delta_\sigma^2)\omega^2 + 16\omega^4\big] + 32\Omega_\sigma^2\big[\gamma_{11}\gamma_{12}(\gamma_{11}^2 + 4\Delta_\sigma^2) + 4(\gamma_{01}\gamma_{11} + 4\Delta_\sigma^2)\omega^2 - 16\omega^4\big] + 256\Omega_\sigma^4(\gamma_{11}^2 + 4\omega^2)}$$

where we use the notation $\gamma_{ij} \equiv i\Gamma + j\gamma_\sigma$ for any integer i, j, with also $\bar{j} \equiv -j$ so, e.g. $\gamma_{35} = 3\Gamma + 5\gamma_\sigma$. The expression is not particularly enlightening but it is completely general, including the Mollow triplet and Heitler regime, at and out-of resonance, also with the effect of detection Γ. An even more complete (with incoherent pumping and dephasing) version of this expression for the 'physical spectrum' of resonance fluorescence is available as a self-standing applet [26]. At any rate, its shape is simple: it is a triplet which maintains a perfect symmetry around the laser frequency set here at $\omega_L = 0$, whose interpretation in the various regimes of driving is given in figure 1*b*,*c*. In both cases, Bohr's insight provides a discerning picture of the otherwise mysterious spectral features of resonance fluorescence. At high-driving, the so-called 'dressed atom' picture considers quantum jumps between the dressed states $|\pm\rangle \equiv c_\pm|g\rangle \pm c_\mp|e\rangle$ of a two-level system $|g\rangle$ and $|e\rangle$ dressed by photons from a driving laser, with $c_\pm \equiv (1 + \xi^{\mp 2})^{-1/2}$ and $\xi \equiv \Omega_\sigma/[\sqrt{\Omega_\sigma^2 + (\Delta_\sigma/2)^2} + (\Delta_\sigma/2)]$. The central peak, at frequency ω_0, is twice as bright as the side peaks $\omega_\pm$ due to two degenerate transitions $|+\rangle \to |+\rangle$ and $|-\rangle \to |-\rangle$. At low driving, now looking at the system in its bare states, a detuned laser does not make it to the excited state and so is restrained chiefly to Rayleigh (energy-conserving) scattering. However, involving two laser photons, one can match the energy ω_σ of the emitter with the excess energy $\omega_\upsilon \equiv 2\omega_L - \omega_\sigma$ (either smaller or larger than ω_σ depending on detuning), forming an exactly symmetric peak. This perceptive physics is well-known since the 1980s, thanks to Reynaud *et al.*'s insights [27–29]. Its understanding has little evolved since then [30].

Since the photoluminescence spectrum is a single-photon observable, one could consider a vanishing detector bandwidth $\Gamma \to 0$ (replacing γ_{ij} by $j\gamma_\sigma$), in which case one sees a tightening of the lines, in particular, the coherent Lorentzian $\lim_{\Gamma\to 0}\mathscr{L}_\Gamma(\omega)$ becomes a Dirac $\delta(\omega)$ function that reflects the vanishing linewidth of the laser treated as a c number (Ω_σ) in equation (2.1).

The effect of detection is thus a mere (and expected) broadening of the lines, which does not qualitatively alter the spectral shape. The case of Heitler resonance ($\Omega_\sigma \ll \gamma_\sigma$ and $\Delta_\sigma = 0$) has attracted deserved but unwary attention. A short discussion will allow us to motivate the significance of detection, to which the sensor formalism gives utmost importance. The spectrum (equation 2.4) reduces in this case to:

$$S_\Gamma(\omega) = \frac{4\Omega_\sigma^2}{\gamma_\sigma^2}\left[\left(1 - \frac{16\Omega_\sigma^2}{\gamma_\sigma^2}\right)\mathscr{L}_\Gamma(\omega) + \frac{8\Omega_\sigma^2}{\gamma_\sigma^2}\frac{2}{\pi}\frac{\gamma_{12}\gamma_{11}^2 + 4\Gamma\omega^2}{(\gamma_{11}^2 + 4\omega^2)^2}\right] \tag{2.7}$$

and, again, the $\Gamma \to 0$ appears to be a straightforward and good-enough approximation of the main features:

$$S_0(\omega) = \frac{4\Omega_\sigma^2}{\gamma_\sigma^2}\left[\left(1 - \frac{16\Omega_\sigma^2}{\gamma_\sigma^2}\right)\delta(\omega) + \frac{8\Omega_\sigma^2}{\gamma_\sigma^2}\pi\gamma_\sigma\mathscr{L}_{\gamma_\sigma}^2(\omega)\right] \tag{2.8}$$

in fact making them particularly transparent, namely, as long as $\Gamma \leq \gamma_\sigma$ (sub-natural linewidth resolution), given that $\Omega_\sigma^2 \ll \gamma_\sigma^2$, the spectrum is essentially a very narrow central line sitting on a weak ($32(\Omega_\sigma/\gamma_\sigma)^4$) and broad ($\gamma_\sigma$) spectrum. This scenario can be seen for the central peak in figure 2*b*. The fluorescent spectrum is, to leading order, the *square* of a Lorentzian, exposing its two-photon origin. This expression corrects the erroneous Eq. (3) in [31]. The impact of the detector in equation (2.7) is merely to contribute a quite innocuous broadening: one can take better and better detectors and converge to the ideal limit equation (2.8), which is essentially $\left(4\Omega_\sigma^2/\gamma_\sigma^2\right)\delta(\omega)$, so it would appear that we are merely discussing technical issues. That is so, at the one-photon level. Two-photon observables, however, behave differently, at least, if taken in their entirety. The complete quantity should retain both the frequencies ω_1 and ω_2 as well as the times of detection t_1 and t_2 of both photons, or, in a steady state, the time difference $\tau = t_2 - t_1$. We will introduce it in the next section, but for now, to compare with the results found in the literature, we assume both frequencies to be that of the emitter $\omega_1 = \omega_2 = \omega_\sigma$, itself at resonance with the laser frequency ω_L, in which case the sensor formalism provides us with $g_\Gamma^{(2)}(\tau) = \left\langle \varsigma_1^\dagger(0)(\varsigma_2^\dagger\varsigma_2)(\tau)\varsigma_1(0)\right\rangle / \left[\left\langle\varsigma_1^\dagger\varsigma_1\right\rangle\left\langle\varsigma_2^\dagger\varsigma_2\right\rangle\right]$ which evaluates to

$$g_\Gamma^{(2)}(\tau) = \left(e^{-(\Gamma+\gamma_\sigma)\tau/2} + \frac{\Gamma\gamma_\sigma}{\Gamma^2 - \gamma_\sigma^2}e^{-\Gamma\tau/2} - \frac{\Gamma^2}{\Gamma^2 - \gamma_\sigma^2}e^{-\gamma_\sigma\tau/2}\right)^2, \tag{2.9}$$

(the limit $\Gamma \to \gamma_\sigma$ gives $g_{\gamma_\sigma}^{(2)}(\tau) = \left[\frac{1+(\gamma_\sigma\tau)/2}{2}e^{-\gamma_\sigma\tau/2} - e^{-\gamma_\sigma\tau}\right]^2$). The most natural way to neglect frequencies is to detect them all, which corresponds to taking the limit $\Gamma \to \infty$, in which case one recovers the result from the literature [32]:

$$g_\infty^{(2)}(\tau) = (1 - e^{-\gamma_\sigma\tau/2})^2. \tag{2.10}$$

This describes an excellent single-photon source (in particular with a flattening $\approx (\gamma_\sigma\tau/2)^2$ at small delays τ around $g^{(2)}(0) = 0$, characteristic of superior single-photon emission [33]). That is to say, one apparently has a bright very narrow—equation (2.8)—and antibunched—equation (2.10)—source. This is thanks to various ingredients contributing their respective benefits: the laser brings the narrow linewidth while the two-level system brings the single-photon emission. But in this listing of great properties, which have been experimentally demonstrated [34,35], one is using different and in fact incompatible configurations, namely, $\Gamma \to 0$ for the spectrum and $\Gamma \to \infty$ for the antibunching. In the laboratory, separate characterizations, overlooking the impact of Γ, have been performed of the system, thereby omitting the crucial adversative conjunction 'or' in describing an 'ultra-coherent or single photon source' [34] and 'subnatural linewidth or single photons' [35]. This oversight shows that Γ is not a mere technical concern but a central consideration. If working directly with equation (2.7) instead of the textbook

limits, then the intrinsic limitations imposed by detection become obvious. The difficulty is that one needs a large enough bandwidth Γ so as to have sufficient integration time to resolve $g^{(2)}(\tau)$ while also having a small enough bandwidth to have a good frequency resolution and not suffer too much broadening. When using the wrong limit for each observable, one indeed gets the worst result possible, namely, $S_\infty(\omega)$ vanishes as the spectrum becomes constant over $(-\infty, +\infty)$ since photons are emitted at all possible frequencies, while $g_0^{(2)}(\tau) = 1$ and all correlations are lost. Uncorrelated emission corresponds in fact to an ideal laser: a physical laser has a linewidth, and filtering below that linewidth goes to the thermal limit $g_0^{(2)}(\tau) = 2$! [36], at any rate, the single-photon correlations are completely lost. Presented in these terms, it would seem that the time/frequency incompatibility occurs at the Fourier level and is thus unavoidable. But this could be easily circumvented merely by replacing the source with one that is more spectrally narrow, i.e. by reducing γ_σ, keeping the same antibunching with a broader-than-natural linewidth of the substitute emitter, but still narrower than the original one: in this way, one can realize arbitrarily narrow and antibunched source, showing that there is no fundamental limitation, only a technical one of finding the suitable emitter. In fact, even the sub-natural linewidth can be realized simultaneously with antibunching, provided a small, but crucial, variation of the experiments [31]. One first needs to understand the nature of antibunching in this system, which, as we said, comes from the two-level system. Or does it? Because driving is weak in this regime, the saturation of the two-level system is not actually needed, in contrast to incoherent excitation where truncation of the number of excitations is crucial. Here, a weak nonlinearity would work as well since the antibunching arises in this case from a two-photon approximation of squeezing antibunching [37] (this is an approximation because there is also three and higher-order antibunching which a squeezed state cannot provide). Squeezing and antibunching have a long shared history of joint appearances, initially with little appreciation of their interconnectedness [17,38,39]. This is in this way that they have been independently theorized [40,41], sought [32,42] and ultimately discovered [43,44] in resonance fluorescence. In such a system, they turn out to be two faces of the same coin, namely, of wave interferences [45]. Interferences are at the heart of both optics and quantum mechanics, so their importance in quantum optics can only be understood as momentous [46,47]. While in classical optics, the simplest waves are described by two parameters—their amplitude and phase—quantum fields come with an infinite number of amplitudes for non-Gaussian states of light, since each multi-photon component $|n\rangle$ of the field $|\psi\rangle = \sum_n c_n |n\rangle$ comes with its own independent coefficient c_n. One can produce rich multi-photon correlated outputs from admixing (or interfering) even the simplest and most popular Gaussian states [48], namely, the coherent state $|\alpha\rangle = \mathscr{D}(\alpha)|0\rangle$, defined in terms of the displacement operator $\mathscr{D}(\alpha) \equiv \exp\left(\alpha a^\dagger - \alpha^* a\right)$ where $\alpha = |\alpha| e^{i\phi}$ and a the harmonic oscillator annihilation operator, so that $(\mathscr{D})^\dagger a \mathscr{D} = a + \alpha$, and the single-mode (quadrature) squeezed state, defined in terms of the squeezing operator $\mathcal{S}_1 \equiv \exp[\frac{1}{2}(\xi^* a^2 - \xi a^{\dagger 2})]$ [49,50]. The idea is as simple as for classical optics interferences: by fine-tuning their respective coefficients, one can realize destructive or constructive interferences for a given component $|n\rangle$ and thus suppress or maximize it in the output. At the Gaussian level, this comes with strong constraints since few parameters define all the multi-photon weights, but because such states are easily produced, they have elicited most of the interest. The idea of admixing squeezing with a coherent state appeared very early, precisely with the aim of producing antibunching [51] (under the name of 'anticorrelation effect'), and in fact even before the more straightforward idea of a two-level system being restored into its ground state [52]. It was then believed that such squeezed anticorrelations might exist in the transient dynamics only. While antibunching from the two-level system was quickly observed [43], the one based on squeezing took more time (and with pulsed excitation) with the signal and pump of a degenerate parametric amplifier, producing both bunching and antibunching by varying the

relative phase [53]. The effect was more clearly understood in terms of two-photon interferences by Lu and Ou [54] who also realized it in the stationary regime. Now that we understand better the origin of antibunching in resonance fluorescence [55] (as squeezing antibunching), we can return to our hope of realizing it simultaneously with a subnatural linewidth. The loss of antibunching [56] in resonance fluorescence is due to the interference between the incoherent and coherent components being disrupted by the detection, which filters out the spectrally broad incoherent (squeezed) fraction more than it does the coherent (narrow) one. One could thus restore antibunching by correcting for this imbalance, which is an excess of coherent state, therefore, destructive interferences with an external laser can achieve that, as was indeed shown theoretically in [31]. Such techniques, that go by the name of 'homodyning', have been demonstrated experimentally to extract the quantum part of a signal [57]. Theoretically, this simply consists in adding a complex field α to the homodyned operator, so σ in our case, i.e. to substitute $\sigma \longrightarrow \alpha + \sigma$ for a tunable $\alpha \in \mathbb{C}$ in the Hamiltonian H_σ. We will go into the details of this mechanism in §4 where we will generalize it to all frequencies of the system, while our current discussion is merely its particular case for photons with the same frequency. For now, it will be enough to note that evidences of such interferences and their effect on the correlations were reported in independent and complementary works that tamper with either the incoherent fraction (and thus loosing antibunching) [55,58] or on the opposite with the coherent fraction (producing excess bunching instead) [59]. Restoring antibunching remains to be demonstrated experimentally. At the theoretical level, our discussion so far should have established that the detection, which manifests itself through the parameter Γ, is at the centre of quantum-optical characterizations and should not be treated lightheartedly. A deep concept is concealed in equation (2.9), namely, that what is being measured is truly the correlations of photons with frequency $\omega_L = 0$, i.e. one is making a complete characterization of both the time and frequency of the photons, which is why Γ is mandatory. What the textbook limit $\Gamma \longrightarrow \infty$ really does is to neglect the frequency information. This is not entirely apparent from equation (2.9) because it seems that no other frequency than the one at which the system emits would make sense anyway. This is not the case. Such a complete description for more general multi-photon observables is discussed in the next section, which embarks us on another departure with the bulk of the literature, this time not for a computational technique only, but at the conceptual level of what it means to detect multi-photons.

3. Frequency-resolved photon correlations

When performing two-photon correlations of the emission from a quantum emitter, there is an irresistible temptation to correlate photons that are 'visible' in the emission spectrum, i.e. that originate from a spectral peak. If the emission further comes in the form of several peaks, that invites for cross-correlating them. This is due to the persistence of the classical picture even to the quantum opticians, despite now many decades of quantum theory telling us that quantum states at the multi-particle level are not conditioned by their attributes at the one-particle level [60]. This makes it conceivable that multi-photon correlations can be more pronounced or interesting in spectral regions where the intensity (or population, i.e. a one-photon observable of the type $\langle a^\dagger a \rangle$) is itself small or even negligible. One must, at the quantum level, separate in principle quantity and quality. It is in fact, beyond conceivable, compulsory to elevate one's understanding of multi-photon emission to such situations where the system does not emit at the one-photon level, but does at the two-photon one, and vice-versa. There can also be joint intense emission of the two types, or jointly suppressed. All combinations are possible. They are therefore conceptually disconnected. To see this, one needs a quantity to visualize two-photon physics, which we now introduce. Such a quantity should have no such prejudice for the spectral peaks, and treat every pair of photons the same. It should be represented on

a two-dimensional plot as it requires two axes, one for each photon. It should also extend or generalize already existing quantities as it is unlikely that the essence of two-photon physics has been missed entirely, although it might well have been left incomplete. Such a two-photon quantity we call the two-photon spectrum [61,62] or two-photon correlation spectrum, which we define in terms of the intensity or population operator $\hat{n}(\omega, t)$ that quantifies the amount of quantum radiation at frequency ω at time t [15], leading to:

$$g^{(2)}_{\Gamma}(\omega_1, \omega_2, t_1, t_2) = \frac{\langle :\hat{n}(\omega_1, t_1)\hat{n}(\omega_2, t_2):\rangle}{\langle \hat{n}(\omega_1, t_1)\rangle\langle \hat{n}(\omega_2, t_2)\rangle}. \tag{3.1}$$

This is a clear generalization of Glauber's two-photon correlation function, but retaining the frequency information along with the temporal one. For this reason, the detector's bandwidth Γ is mandatory. This quantity has been considered by various authors [63–65], but it has presented considerable difficulties and only partial results could be derived, sometimes with inconsistencies. From the sensor formalism, however, it is easily and exactly obtained as

$$g^{(2)}_{\Gamma}(\omega_1, \omega_2, t_1, t_2) = \frac{\left\langle \varsigma_1^{\dagger}(t_1)(\varsigma_2^{\dagger}\varsigma_2)(t_2)\varsigma_1(t_1)\right\rangle}{\left\langle (\varsigma_1^{\dagger}\varsigma_1)(t_1)\right\rangle\left\langle (\varsigma_2^{\dagger}\varsigma_2)(t_2)\right\rangle}. \tag{3.2}$$

While one can consider both time and frequency (e.g. [66,67]), it will be enough for the present text to consider coincidences of a stationary state, i.e. the case $t_1 = t_2 \to \infty$. This will not diminish the main insight that in so doing, we are making a joint characterization in time (albeit coincidences only) and frequencies. We now embrace the full picture and compute numerically two-frequency coincidences (equation 3.2) through standard quantum averages of the sensor method. Since frequencies are mere parameters, this allows a convenient and exact computation of what was previously obtained at the cost of great efforts and several oversimplifying approximations [68,69]. The results are shown in figure 2*d–f* (second row), below the corresponding spectral shapes, reproducing three notable cases from the pioneering work [62]. Unlike the top row, where $S_{\Gamma}(\omega)$ could be obtained in the limit $\Gamma \to 0$, these two-photon spectra would become 'trivial' in this limit, with $g^{(2)}_{0}(\omega_1, \omega_2) = 1$, i.e. washing out all traces of correlations as the detectors integrate over infinite times. The other limit is more interesting but brings nothing new as it recovers equation (2.10), and so, at $\tau = 0$, is identically zero. What is of interest, clearly, is the intermediate case where a landscape of correlations is revealed. It will be enough to limit ourselves with a description of the qualitative features, although we repeat that the results are numerically exact, so one could study cross-sections in more quantitative details. In our qualitative description, red colours correspond to bunching, i.e. to photons with the respective frequencies arriving together in time, with antidiagonals of bunching in cases (*d*) and (*e*) that correspond to the two-photon Mollow triplet. These lines indeed generalize Bohr's quantization condition for transitions between two energies $E_i - E_j = \omega$, to a two-photon jump

$$E_k - E_l = \omega_1 + \omega_2 \tag{3.3}$$

where the energies E_k and E_l are non-contiguous in the energy ladder and so the system effectively 'jumps over' a real state, for which reason this has been termed a leapfrog process [61,62]. This is the direct quantum-optical counterpart of Göpert Mayer's Doppelemission with a few but important variations. In her case, there was nothing to jump over, and the multi-photon emission was thus in a different frequency range, indeed, in its manifestation from nebulae emission, this converts UV $2S \to 1S$ Lyman photons into the visual continuum siding with the visible Balmer series $X \to 2S$. Higher order processes fall into still more remote spectral windows, while our leapfrog processes, even from three or a higher number of photons, are all over the place along with the single photons that one sees in the spectral shape. The second variation is our reliance on the quantum-optical quantity $g^{(2)}_{\Gamma}(\omega_1, \omega_2)$ (this would be $g^{(n)}$ for higher

photon numbers), which allows us to 'reveal' this hitherto unsuspected structure, whose existence is, again, not conditioned to the amount of signal, and can be captured by using an adequate two-photon observable, which, as Glauber clarified for quantum light, is the intensity–intensity correlator [60]. As a result, one should look for such multi-photon emission everywhere, not only when it is betrayed, for one reason or another, at the one-photon level. In most cases, it remains invisible (at the one photon level). The appropriate photon correlations allow us to extract them from a background of unrelated or more intense emission. Another variation is that, two-photon light being more complex than single-photon light, it comes with more characteristics, which we capture with colours in addition to a magnitude. Besides red for bunching, we use white for uncorrelated emission, where the two photons are emitted independently the one from the other. Interestingly, one can see in figure 2*d* that such uncorrelated photons form a grid of horizontal and vertical lines defined by the (one-photon) spectral peaks. This means that photons from the spectral peaks contribute not only the bulk, indeed, of the emission, but more significantly, the classical signal, which is independent from the rest of the emission. This is another call for quantum opticians to seek their photons away from the peaks: quantum photons are emitted where one does not seem them. This is because photons from the spectral peaks are 'real' photons that arise from the Bohrian jump from one real (here, dressed) state to another, while leapfrog photons are virtual, in the sense that they involve a virtual intermediate state with energy E_l^* which could be any value in between or even beyond, and thus resulting in a correlated signal for the entire line satisfying equation (3.3). Virtual does not mean 'non-existing' and would one still complain of no emission from outside the peaks, we would retort again that this is a one-photon concern. The no-emission at the two-photon level is unrelated to no-emission at the one-photon one. No two-photon emission is in fact what we encode with the blue colour in the two-photon spectrum, for antibunching. And one can see in figure 2*d* how the strongest no two-photon emission occurs at $(\varpi_1, \varpi_2) = (-1, -1)$ or $(+1, +1)$, i.e. at the spectral side peaks, where one-photon emission is indeed strong. Such a scenario is well known, as it corresponds to single-photon emission. In contrast, at $(\varpi_1, \varpi_2) = \frac{1}{2}(-1, -1)$ or $\frac{1}{2}(+1, +1)$, one has the opposite situation of strong two-photon emission but small one-photon emission (in fact the smallest emission in the range $|\varpi| \lessapprox 1.25$), which corresponds to the equally fundamental case of two-photon leaprog emission, which may be even more important than single-photon emission, although, because it is innocuous at the one-photon level, it failed to attract much attention so far. One must highlight in this regard the exceptional contributions from the beautiful and still unique experiments of the Muller group [70–73], who has observed these features in spectacular agreement with the theory. Finally, a manifestation of the independent yet tangible existence of the two-photon physics can be based on arguments of theoretical aesthetics: the robust spectral (one-photon) symmetry with detuning, which appears to be lifted at the two-photon level since the two peaks behave differently in the two-photon spectrum, is instead 'rotated': the symmetry is with respect to the two-photon diagonal, so independent from the one-photon structure, but also present when looked at properly. This needed change of perspective, we believe, is an evidence of the independent two-photon picture. If such arguments fail to move one's sensibility, and although we are focused on the fundamental aspects in this text, we should then mention that there are obvious and immediate technological prospects of these results that turn the correlated virtual photons into quantum emission of a new type. For instance, placing a cavity at the N-photon leapfrog degenerate frequency (halfway between the peaks for two photons) would Purcell-enhance their emission and open a bright channel of pure N-photon emission [74]. This is clearly another evidence of the 'existence' of such processes, that can power devices of a new type. There are other ways to similarly exploit this hidden

physics, but we wish to return instead to its basic structure, and now focus on the perplexing blue circle cast between the central and virtual peaks, as seen in figure 2*f*. This circle is of a different nature from the phenomenology that we have discussed so far, since this is a curve as opposed to straight lines, and suppressing photons instead of having them come together as joint emission. We now explain here for the first time the underlying mechanism for this circle.

4. Admixing two-mode squeezed and coherent states

Two-photon physics is primarily described by Fock states $|2\rangle$ in a given mode, or by non-degenerate pairs $|1_1 1_2\rangle$ in two modes. Next come the so-called *squeezed states*, which were popularized by Walls [75] for their ability to squeeze through the uncertainty principle [76], but were initially (and possibly, more appropriately) called 'two-photon coherent states' by Yuen [77]. Because two-photon spectra correlate two frequencies (providing two continuously varying modes), two-mode squeezing can be expected to have some relevance in the presence of coherence, as is the case for resonance fluorescence which involves coherent driving. Two-mode squeezing considers two bosonic modes with annihilation operators a_1 and a_2, and a so-called 'squeezing matrix' ζ_{ij} (complex-valued symmetric). The two-mode squeezing operator [78]

$$\mathcal{S}_2^{(ij)} = \exp[\zeta_{ij} a_i a_j - \zeta_{ij}^* a_i^\dagger a_j^\dagger], \tag{4.1}$$

can be seen as a generalization of the already introduced single-mode squeezing operator

$$\mathcal{S}_1^{(i)} = \exp[\frac{1}{2}(\xi_i^* a_i^2 - \xi_i a_i^{\dagger 2})], \tag{4.2}$$

where the squeezing parameters are conveniently defined as $\xi_i = r_i e^{i\vartheta_i}$ for $i = 1, 2$ and $\zeta_{ij} = t_{ij} e^{i\vartheta_{ij}}$ a matrix with zero diagonal elements, namely $\zeta_{12} = t_{12} e^{i\vartheta_{12}}$ with $\zeta_{jj} = 0$ for $j = 1,2$. One can squeeze the two modes independently, with the product of the single-mode squeezing operators $\mathcal{S}_1^{(1)}(\xi_1)\mathcal{S}_1^{(2)}(\xi_2) = \mathcal{S}_1^{(2)}(\xi_2)\mathcal{S}_1^{(1)}(\xi_1)$ (the operators commute), or squeeze them jointly with the two-mode squeezing operator $\mathcal{S}_2^{(12)}(\zeta_{12})$, transforming annihilation operators as [78]:

$$(\mathcal{S}_2^{(12)})^\dagger a_i \mathcal{S}_2^{(12)} = \sum_{k=1,2} \left(\mathcal{M}_{ik} a_k - \mathcal{N}_{ik} a_k^\dagger \right), \tag{4.3}$$

for $1 \le i \le 2$. The mixing matrix $\mathcal{M}$ is positive while the second mixing matrix $\mathcal{N}$ can be complex-valued. For single-mode squeezing, they are diagonal with values $\mathcal{M}_{ii} = \cosh(r_i)$ and $\mathcal{N}_{ii} = e^{i\vartheta_i}\sinh(r_i)$, respectively. On the other hand, for two-mode squeezing, the non-vanishing elements are $\mathcal{M}_{11} = \mathcal{M}_{22} = \cosh(t_{12})$ and $\mathcal{N}_{12} = \mathcal{N}_{21} = e^{i\vartheta_{12}}\sinh(t_{12})$. This leads to the transformation rules for the one- and two-mode operators:

$$(\mathcal{S}_1^{(i)})^\dagger a_i \mathcal{S}_1^{(i)} = \mu_i a_i - \nu_i a_i^\dagger \quad \text{and} \quad (\mathcal{S}_2^{(12)})^\dagger a_i \mathcal{S}_2^{(12)} = \mathcal{M}_{11} a_i - \mathcal{N}_{12} a_{\bar{\imath}}^\dagger, \tag{4.4}$$

where $\mu_i = \cosh(r_i)$, $\nu_i = e^{i\vartheta_i}\sinh(r_i)$, $\mathcal{M}_{11} = \cosh(t_{12})$, $\mathcal{N}_{12} = e^{i\vartheta_{12}}\sinh(t_{12})$ and $\bar{\imath} \equiv 3 - i$ exchanges 1 and 2. Alternatively, one could use the general form of $\mathcal{S}_2^{(12)}$, with structurally identical results. The combination of these squeezings leads to a generic two-mode squeezed state:

$$|\xi_1, \xi_2, \zeta_{12}\rangle \equiv \mathcal{S}_1^{(1)}\mathcal{S}_1^{(2)}\mathcal{S}_2^{(12)}|0\,0\rangle. \tag{4.5}$$

For this state, it is straightforward to compute any correlator $\langle a_1^{\dagger m} a_1^n a_2^{\dagger p} a_2^q \rangle$ for integers m, n, p, q from equation (4.3). For instance, we find for the population of mode $i = 1,2$:

$$\langle a_i^\dagger a_i \rangle = \cosh^2 r_i \sinh^2 t + \sinh^2 r_i \cosh^2 t\,. \tag{4.6}$$

One could carry on like this and compute other correlators but since we shall be concerned in the following with leading-order processes, we can rescale the squeezing parameters as $r_i \to \epsilon^2 r_i$ and $t \to \epsilon^2 t$ for an ϵ that will be taken close to zero. In this limit, thanks to normalization, we can give a more comprehensive list of the correlators, including the second-order correlation functions $g_i^{(2)} \equiv \langle a_i^{\dagger 2} a_i^2 \rangle / \langle a_i^\dagger a_i \rangle^2$ for $i = 1,2$ and $g_{12}^{(2)} \equiv \langle a_1^\dagger a_2^\dagger a_2 a_1 \rangle / \langle a_1^\dagger a_1 \rangle \langle a_2^\dagger a_2 \rangle$:

$$\langle a_i^\dagger a_i \rangle \approx \left(r_i^2 + t_{12}^2\right)\epsilon^4\,, \qquad \langle a_1 a_2 \rangle \approx -\epsilon^2 \zeta_{12}\,, \qquad \langle a_i^2 \rangle \approx -\epsilon^2 \xi_i\,, \tag{4.7a}$$

$$g_i^{(2)} \approx \frac{r_1^4}{(r_1^2 + t_{12}^2)(r_2^2 + t_{12}^2)\epsilon^4}\,, \qquad g_{12}^{(2)} \approx \frac{t_{12}^4}{(r_1^2 + t_{12}^2)(r_2^2 + t_{12}^2)\epsilon^4}\,. \tag{4.7b}$$

Since ϵ is very small, one can see that all the two-particle fluctuations are bunched. We can, however, produce antibunching by interfering squeezing with a coherent state, as we already discussed for the Heitler regime at resonance. Here, we will look more closely at the general case of interferences that involve two-mode squeezing, and show that this captures much of the two-photon physics of resonance fluorescence. This extends to two modes the idea already scrutinized for one mode [16,31], which admixture of coherence with squeezing results in rich and qualitatively different correlations than those available in the squeezed or coherent states alone. This should similarly allow us to generalize the specific technique of tuning photon statistics with coherent fields [48] to multi-mode correlations, especially as multi-mode coherent states are not correlated, so they can be tuned independently for each squeezed mode. From the weak driving that defines resonance fluorescence, it is enough to deal with coherent-squeezed states in the limit of small squeezing. Since the coherent contribution of the quantum states is taken of the same order than squeezing, we take $\alpha_i \to \epsilon\,\alpha_i$, meaning, however, that coherence is stronger since it appears to first order in the admixture while squeezing is of second order. This brings us to the fundamental object of two-photon resonance fluorescence:

$$|\boldsymbol{\alpha}, \boldsymbol{\xi}, \zeta_{12}\rangle \equiv \mathscr{D}_1 \mathscr{D}_2\, \mathcal{S}_1^{(1)} \mathcal{S}_1^{(2)} \mathcal{S}_2^{(12)} |0\,0\rangle, \tag{4.8}$$

where $\boldsymbol{\alpha} \equiv (\alpha_1, \alpha_2)$ and $\boldsymbol{\xi} \equiv (\xi_1, \xi_2)$ admixes coherence and squeezing of single modes [48] along with ζ_{12} that provides the general two-photon physics. Similarly as before, we can now compute the key two-photon correlators for this state, to leading order in ϵ:

$$\langle a_i^\dagger a_i \rangle \approx \epsilon^2 |\alpha_i|^2 + \epsilon^4 \left\{ t_{12}^2 + r_i^2 - 2|\alpha_i|^2 r_i \cos(2\phi_i - \theta_i) - 2|\alpha_1||\alpha_2| t_{12} \cos(\phi_1 + \phi_2 - \vartheta_{12}) \right\}, \tag{4.9a}$$

$$\langle a_i^2 \rangle \approx \epsilon^2 \left(\alpha_i^2 - \xi_i\right), \quad \langle a_1 a_2 \rangle \approx \epsilon^2 (\alpha_1 \alpha_2 - \zeta_{12})\,, \tag{4.9b}$$

$$g_i^{(2)} \approx 1 - \frac{2\, r_i \cos(2\phi_i - \theta_i)}{|\alpha_i|^2} + \frac{r_i^2}{|\alpha_i|^4}\,, \tag{4.9c}$$

$$g_{12}^{(2)} \approx 1 - \frac{2\, t \cos(\phi_1 + \phi_2 - \vartheta_{12})}{|\alpha_1||\alpha_2|} + \frac{t_{12}^2}{|\alpha_1|^2 |\alpha_2|^2}\,, \tag{4.9d}$$

for $1 \le i, j \le 2$. As compared with equation (4.7), one can see that the correlators $g^{(2)}$ can now take a much wider span of possible values, in particular, they can now be less than unity and even vanish exactly as well as diverge to leading order. This is the two-mode generalization of our previous single-mode admixing [48], where it was also the case that the population, equation (4.9*a*), is essentially coherent, since $\epsilon^2 \gg \epsilon^4$, but that, regardless of this preponderance of the coherent state, two-photon observables are ruled by the squeezing component. Here too,

the intensity of the squeezed photons has to be much smaller than the coherent one. The reason is that in order to interfere at the two-photon level (to produce antibunching), the contributions have to be of the same order, what we have achieved thanks to the parametrization. The coherent field makes the system gain one photon, with a probability proportional to $|\alpha_i|$. To climb up from vacuum to $|2\rangle$, the system has to absorb two photons, one each time, so the chances are proportional to $|\alpha_i|^2$. On the other hand, the squeezed field carries the photons two by two. Then, the system can directly jump from $|0\rangle$ to $|2\rangle$ by absorbing two photons with a probability proportional to r_i. To ensure that both processes compete on equal footing, the ratio $|\alpha_i|^2/r_i$ has to remain finite when the limits $|\alpha_i|, r_i \to 0$ are taken. For the two-mode case, the interference yields the cancellation of the $|1,1\rangle$ state and the argument is exactly the same just exchanging $|\alpha_i|^2 \to |\alpha_1||\alpha_2|$ and $r_i \to t_{12}$. This explains the counter-intuitive fact that a weak incoherent fraction determines the antibunching of an intense coherent radiation [31,55]. A major departure from two-mode squeezing as compared with single-mode admixing is the degeneracy for the conditions that realize interferences and produce extreme correlations, such as perfect antibunching (exact zero) or diverging superbunching. Indeed, perfect anticorrelation for a single mode is obtained when these conditions are fulfilled:

$$r_i = |\alpha_i|^2, \qquad 2\phi_i - \theta_i = 0, \tag{4.10}$$

while two-mode anticorrelations are maximized when:

$$t_{12} = |\alpha_1\alpha_2|, \quad \phi_1 + \phi_2 - \vartheta_{12} = 0. \tag{4.11}$$

Just like two-photon leapfrog transitions (cf. §3) lift the strict conservation of energy for each photon to constrain their sum instead—allowing each photon in the pair to come with a continuous energy [62,67]—here, the wave interference is realized for a sum of the phases, in contrast to the single phase for a single mode [16]. This allows, again, a continuous range of parameters to realize the quantum interference. Such admixtures can also be tracked in any dynamical two-mode quantum state, possibly mixed with a density matrix ρ. We will consider explicitly the case of resonance fluorescence, which is the simplest one, but of course our discussion is general, whether the coherence is provided internally (as is the case in resonance fluorescence where it is inherited from the coherent driving) or is added externally, with a supplementary (homodyning) laser, a case we shall also touch upon. It could also be developed by the system itself (e.g. when it undergoes lasing). Whatever the origin for the various contributions, one can separate them from the whole operators a_i that act on the whole state from those $\tilde{a}_i$ that act only on the fluctuations, or incoherent part. They are linked by the relation

$$a_i = \alpha_i + \tilde{a}_i \tag{4.12}$$

where again a_i and $\tilde{a}_i$ are operators while α_i is a c-number. This again generalizes our earlier case [48] and while we limit ourselves here to $i = 1,2$, one could further extend it to any number of modes. By construction, one has $\langle\tilde{a}_i\rangle = 0$, resulting in no interferences for the intensities: $\langle a_i^\dagger a_i\rangle = |\alpha_i|^2 + \langle\tilde{a}_i^\dagger\tilde{a}_i\rangle$. In stark contrast, the cross-correlator $\langle a_1^\dagger a_2^\dagger a_2 a_1\rangle$ becomes

$\langle(\tilde{a}_1^\dagger + \alpha_1^*)(\tilde{a}_2^\dagger + \alpha_2^*)(a_2 + \alpha_2)(a_1 + \alpha_1)\rangle$. Expanding this, we get:

$$\begin{aligned}\langle a_1^\dagger a_2^\dagger a_2 a_1\rangle = \langle\tilde{a}_1^\dagger\tilde{a}_2^\dagger\tilde{a}_2\tilde{a}_1\rangle + \sum_{i=1,2}\left(\alpha_i\langle\tilde{a}_1^\dagger\tilde{a}_2^\dagger\tilde{a}_{\bar{i}}\rangle + \mathrm{cc}\right) \\ + \left(\alpha_1\alpha_2\langle\tilde{a}_1^\dagger\tilde{a}_2^\dagger\rangle + \alpha_1\alpha_2^*\langle\tilde{a}_1^\dagger\tilde{a}_2\rangle + \mathrm{cc}\right) + \sum_{i=1,2}|\alpha_i|^2\langle\tilde{a}_i^\dagger\tilde{a}_i\rangle\end{aligned} \tag{4.13}$$

where, again, $\bar{\imath} \equiv 3 - i$. This shows that, unlike incoherent intensities, the second-order correlation functions are the result of interferences, namely, of four terms:

royalsocietypublishing.org/journal/rsta Phil. Trans. R. Soc. A 382: 20230315

$$g^{(2)}_{12} = 1 + \mathcal{I}_0 + \mathcal{I}_1 + \mathcal{I}_2, \tag{4.14}$$

with

$$\mathcal{I}_0 \equiv \frac{1}{n_1 n_2}\left\{\langle \tilde{a}_1^\dagger \tilde{a}_2^\dagger \tilde{a}_2 \tilde{a}_1\rangle - \langle \tilde{a}_1^\dagger \tilde{a}_1\rangle\langle \tilde{a}_2^\dagger \tilde{a}_2\rangle\right\}, \tag{4.15a}$$

$$\mathcal{I}_1 \equiv \frac{2}{n_1 n_2}\mathrm{Re}\left\{\alpha_1\langle \tilde{a}_1^\dagger \tilde{a}_2^\dagger \tilde{a}_2\rangle + \alpha_2\langle \tilde{a}_1^\dagger \tilde{a}_2^\dagger \tilde{a}_1\rangle\right\}, \tag{4.15b}$$

$$\mathcal{I}_2 \equiv \frac{2}{n_1 n_2}\mathrm{Re}\left\{\alpha_1\alpha_2\langle \tilde{a}_1^\dagger \tilde{a}_2^\dagger\rangle + \alpha_1\alpha_2^*\langle \tilde{a}_1^\dagger \tilde{a}_2\rangle\right\}, \tag{4.15c}$$

with $n_i \equiv \langle a_i^\dagger a_i\rangle$ so that in each case, $\mathcal{I}_i n_1 n_2$ is of order $|\alpha_1|^p|\alpha_2|^q$ with $p+q=i$. We now have recovered the general version of the phenomenon discussed in §2 of antibunching produced by an interference of various contributions, which are the single-mode version of $\mathcal{I}_i$, i.e. with $a_1 = a_2 = a$, in which case $\mathcal{I}_0$ is related to the $g^{(2)}$ of the incoherent fraction, being −1 for non-Gaussian (quantum) antibunching and +1 for chaotic, bunched states, while $\mathcal{I}_2$ is related to squeezing, being −2 in the presence of squeezing. $\mathcal{I}_1$ is a measure of anomalous moments which is negligible in the two regimes of interest, namely:

- Heitler regime, where $g^{(2)} = 0 = 1 + (\mathcal{I}_0 = 1) + (\mathcal{I}_1 = 0) + (\mathcal{I}_2 = -2)$,
- Mollow regime, where $g^{(2)} = 0 = 1 + (\mathcal{I}_0 = -1) + (\mathcal{I}_1 = 0) + (\mathcal{I}_2 = 0)$,

with, therefore, a completely different interpretation for how $g^{(2)} = 0$ is obtained. In the general case that we consider here, the numerator of $\mathcal{I}_1$ has the physical meaning of a covariance between the incoherent fractions, being positive when both modes are occupied or depleted together, and negative when one is largely occupied and the other depleted. Like for the single mode, the normalization is to the *total* population, not to that of the incoherent fraction alone. $\mathcal{I}_2$ also has some interpretation in terms of two-mode squeezing, in particular including the coherent fractions α_1 and α_2. We shall disregard the exact meaning of $\mathcal{I}_1$ that interpolates between the various regimes by involving anomalous correlators of the populations and order parameters of the type $\langle \tilde{a}_i^\dagger \tilde{a}_i \tilde{a}_i\rangle$, also weighted by the coherent fraction α_i^*. We can also write these expressions not for the quantum fields only (fluctuations), but for the full-state correlators, which might be more accessible either experimentally or theoretically. To do so, we can use the backward relation:

$$\langle \tilde{a}_1^{\dagger i}\tilde{a}_2^{\dagger j}\tilde{a}_2^k\tilde{a}_1^l\rangle = \sum_{i',j',k',l'=0}^{i,j,k,l}(-1)^{i'+j'+k'+l'}\binom{i}{i'}\binom{j}{j'}\binom{k}{k'}\binom{l}{l'}(\alpha_1^*)^{i-i'}(\alpha_2^*)^{j-j'}\alpha_2^{k'}\alpha_1^{l'}\times \langle a_1^{\dagger(i-i')}a_2^{\dagger(j-j')}a_1^{k-k'}a_2^{l-l'}\rangle, \tag{4.16}$$

which applied to $\mathcal{I}_i$ leads to:

$$\mathcal{I}_0 = \Big(\langle a_1^\dagger a_2^\dagger a_2 a_1\rangle - \langle a_1^\dagger a_1\rangle\langle a_2^\dagger a_2\rangle - 4\,|\alpha_1|^2|\alpha_2|^2 + 2\,|\alpha_1|^2\langle a_2^\dagger a_2\rangle + 2\,|\alpha_2|^2\langle a_1^\dagger a_1\rangle + 2\,\mathrm{Re}\left\{\alpha_1\alpha_2\langle a_1^\dagger a_2^\dagger\rangle + \alpha_1\alpha_2^*\langle a_1^\dagger a_2\rangle - \alpha_1\langle a_1^\dagger a_2^\dagger a_2\rangle - \alpha_2\langle a_1^\dagger a_2^\dagger a_1\rangle\right\}\Big)/n_1 n_2, \tag{4.17a}$$

$$\mathcal{I}_1 = 2\,\mathrm{Re}\Big(\alpha_1\langle a_1^\dagger a_2^\dagger a_2\rangle + \alpha_2\langle a_1^\dagger b^\dagger a_1\rangle - 2\,\alpha_1\alpha_2\langle a_1^\dagger a_2^\dagger\rangle - 2\,\alpha_1\alpha_2^*\langle a_1^\dagger a_2\rangle + 2\,|\alpha_1|^2|\alpha_2|^2 - |\alpha_1|^2\langle a_2^\dagger a_2\rangle - |\alpha_2|^2\langle a_1^\dagger a_1\rangle\Big)/n_1 n_2, \tag{4.17b}$$

$$\mathcal{I}_2 = 2\,\mathrm{Re}\Big(\alpha_1\alpha_2\langle a_1^\dagger a_2^\dagger\rangle + \alpha_1\alpha_2^*\langle a_1^\dagger a_2\rangle - 2\,|\alpha_1|^2|\alpha_2|^2\Big)/n_1 n_2\,. \tag{4.17c}$$

One can recover from this general result the particular case in equation (4.8) of a coherent squeezed state by checking that these quantities for $|\boldsymbol{\alpha}, \boldsymbol{\xi}, \zeta_{12}\rangle$ with vanishing amplitudes ($\alpha_i \to \epsilon\alpha_i$, $r_i \to \epsilon^2 r_i$ and $t_{12} \to \epsilon^2 t_{12}$, with $\epsilon \to 0$), read

$$\mathcal{I}_0 \approx \frac{t_{12}^2}{|\alpha_1|^2\,|\alpha_2|^2}, \qquad \mathcal{I}_2 \approx -\frac{2t_{12}\cos(\phi_1+\phi_2-\vartheta_{12})}{|\alpha_1|\,|\alpha_2|}, \tag{4.18}$$

while the anomalous $\mathcal{I}_1$ is exactly zero for any set of parameters. This recovers equation (4.9*d*) from equation (4.14) and, with the conditions for the cancellation of $g_{12}^{(2)}$ in equation (4.11), this gives

$$\mathcal{I}_0 \approx 1, \qquad \mathcal{I}_2 \approx -2, \tag{4.19}$$

i.e. it is the compensation between the mean field and the squeezed two-mode fluctuations that leads to $g_{12}^{(2)} = 0$ at first order in the parameters, just as we find for single-mode antibunching [48,55]. All the previous considerations would be interesting, but formal results only, would it not be for the link that photodetection offers to the theory of frequency-resolved photon correlations, as discussed in §3. Namely, retaining the frequency information of the photons that one correlates, brings to the fore the decomposition equation (4.18) but now for the continuously varying frequencies ω_i as opposed to independent modes a_i. We now turn to such a dynamical setting.

5. Squeezed cavity

We return to the two-photon spectrum, to reveal how the concepts of squeezed and coherent admixtures introduced in §4 explain the results we reported for resonance fluorescence in figure 2. We can best show that this is the case by bringing directly all these components externally to a cavity a and collect the re-emitted admixed light, instead of a two-level system producing them internally. This approach also invites closer inspection of such excitation schemes [79]. The sensor technique for this scenario produces the Hamiltonian:

$$H_a = \Delta_a\, a^\dagger a + i\frac{\Lambda_a}{2}(a^{\dagger 2} - a^2) + \Omega_a(e^{i\vartheta}a^\dagger + e^{-i\vartheta}a) + \Delta_1\varsigma_1^\dagger\varsigma_1 + \Delta_2\varsigma_2^\dagger\varsigma_2 + \epsilon\sum_{i=1,2}(a^\dagger\varsigma_i + \varsigma_i^\dagger a). \tag{5.1}$$

Here, we have a passive, linear cavity a, driven by both a squeezed source with strength Λ_a and a laser with amplitude Ω_a, with ϑ the phase difference between the coherent and squeezed sources. In resonance fluorescence, only the coherent state is provided externally while the weak nonlinearity, given the weak driving, produces the squeezing. In other cases, everything could be produced by the system itself (e.g. like the Mollow triplet produced under incoherent pumping when placed in a cavity that undergoes lasing [80]). While the two-level system is inherently antibunched ($g_\sigma^{(2)}(0) = 0$), independent of the nature and strength of the driving, a squeezed coherent cavity may modulate the photon statistics from bunched to antibunched as the parameters change. As we are interested in showing the similarity of this system with resonance fluorescence, we first seek to find the conditions that minimize the cavity's two-photon correlator $g_a^{(2)}$. In the steady-state, the bare correlations of the squeezed cavity are

$$\langle a\rangle = -\frac{2i\Omega_a[e^{i\vartheta}(\gamma_a - 2i\Delta_a) - 2e^{-i\vartheta}\Lambda_a]}{\gamma_a^2 + 4\Delta_a^2 - 4\Lambda_a^2} \quad \text{and} \quad \langle a^\dagger a\rangle = \frac{2\Lambda_a^2}{\gamma_a^2 + 4\Delta_a^2 - 4\Lambda_a^2} + |\langle a\rangle|^2. \tag{5.2}$$

We do not provide the expression for the general $g_a^{(2)}$ as it is too voluminous and not immediately needed for our discussion, unlike the variance $\langle a^2\rangle - \langle a\rangle^2 = \Lambda_a(\gamma_a - 2i\Delta_a)/[\gamma_a^2 + 4\Delta_a^2 - 4\Lambda_a^2]$ that is required for the phase matching $\theta = 2\phi$ between $\phi \equiv \arg(\langle a\rangle)$ and $\theta \equiv \arg(\langle a^2\rangle - \langle a\rangle^2)$

needed to minimize $g_a^{(2)}$. This is satisfied for $\tan(2\vartheta) = 2\Delta_a/\gamma_a$. There is an upper-bound for the squeezing amplitude Λ_a beyond which the system is unstable and results in unphysical steady states, namely, it must be that $\Lambda_a < \sqrt{\gamma_a^2 + 4\Delta_a^2}/2$. Reparameterizing Λ_a as $\Lambda_a = \Gamma_a\lambda/2$ where $\Gamma_a \equiv \sqrt{\gamma_a^2 + 4\Delta_a^2}$, expresses this stability condition to $\lambda < 1$. The cavity phase and its population in the phase-matching, i.e. optimum antibunching configuration, are then found as

$$\langle a\rangle = \frac{2i\Omega_a\sqrt{\gamma_a - 2i\Delta_a}}{(1+\lambda)\Gamma_a^3} \quad \text{and} \quad \langle a^\dagger a\rangle = (1+\lambda)^{-2}\left[\frac{4\Omega_a^2}{\Gamma_a^2} + \frac{\lambda^2(1+\lambda)}{2(1-\lambda)}\right], \tag{5.3}$$

with now a tractable two-photon coincidences phase-matched $g_a^{(2)}$ (in the $\Gamma \to \infty$ limit):

$$g_a^{(2)}(0) = \frac{(1-\lambda)^2}{[\Gamma_a^2\lambda^2(\lambda^2-1) - 8\Omega_a^2(1-\lambda^2)]^2}\left[\Gamma_a^4\lambda^2(1+\lambda)^2(1+2\lambda^2) + 16\Omega_2^2\Gamma_a^2\lambda(\lambda^2-1)(1-2\lambda) + 64(1-\lambda)^2\Omega_a^4\right]. \tag{5.4}$$

Deriving equation (5.4) with respect to Ω_a, we find the minimum value possible for $g_a^{(2)}$ of a squeezed cavity admixed to a coherent state:

$$g_{a,\min}^{(2)} = 2\frac{\lambda(2-\lambda)}{1+2\lambda-\lambda^2} \overset{\lambda \to 0}{\approx} 0 + 4\lambda\,, \tag{5.5}$$

which is obtained for the 'optimum' driving $\Omega_{a,\,\mathrm{optmin}}$:

$$\Omega_{a,\,\mathrm{optmin}} = \frac{\Gamma_a\sqrt{\lambda/2}(1+\lambda)}{2(1-\lambda)} \overset{\lambda \to 0}{\approx} \frac{\Gamma_a}{2}\sqrt{\lambda/2}\,. \tag{5.6}$$

This produces antibunching for the whole range $0 \le \lambda < 1$ and reaches zero as λ gets smaller (for both $\Lambda_a \to 0$ and $\Delta_a \to \infty$, which is the case of interest). Applying the optimum antibunching conditions in the limiting case $\Delta_a \to \infty$ and, therefore $\lambda \to 0$, we get for the spectrum

$$S_{a,\Gamma}(\omega) \approx |\langle a\rangle|^2\mathscr{L}_\Gamma(\omega) + (\langle a^\dagger a\rangle - |\langle a\rangle|^2)\frac{2}{\pi}\frac{\gamma_{12}(\gamma_{11}^2 + 4\Delta_a^2) + 4\Gamma\omega^2}{(\gamma_{11}^2 + 4\omega^2)^2 + 8\Delta_a^2(\gamma_{11}^2 - 4\omega^2) + 16\Delta_a^4} \tag{5.7}$$

where we also used the shortcut $\gamma_{ij} \equiv i\Gamma + j\gamma_a$ but this time for γ_a. We will now show that this matches exactly the two-level system result. The same occurs for the two-photon correlator for the squeezed cavity,

$$g_a^{(2)}(\tau) \approx 1 + e^{-\gamma_a\tau} - 2\,e^{-\gamma_a/2\,\tau}\cos(2\Delta_a\tau)\,, \tag{5.8}$$

which is identical at resonance to the expression for the unfiltered two-level system, cf. equation (2.10). In the next section, we show that the agreement holds also in the presence of detuning. We conclude this preliminary section with the numerically exact two-photon spectrum for the squeezed cavity in the optimum phase-matching, $\theta = 2\phi$, and pumping, equation (5.6), conditions, which is shown in figure 3*a*. Its excellent qualitative agreement for most of the features with resonance fluorescence involving the two-level system, is obvious (cf. figure 2*f*). This confirms the central importance of quantum state interferences in general and of coherent and squeezed states in particular, to account for the phenomenology of two-photon physics of detuned resonance fluorescence. This is fully established in the next section.

6. Detuned resonance fluorescence

We can now complete our argument by returning to the two-photon spectrum of resonance fluorescence (i.e. for the two-level system σ). We will focus on detuning, since this highlights various features of interest, starting with the spectral separation of the coherent peak, which stays pinned at the centre, from the incoherent emission, that splits into the symmetric doublet of side peaks, with a neat interpretation in terms of two-photon scattering as sketched in figure

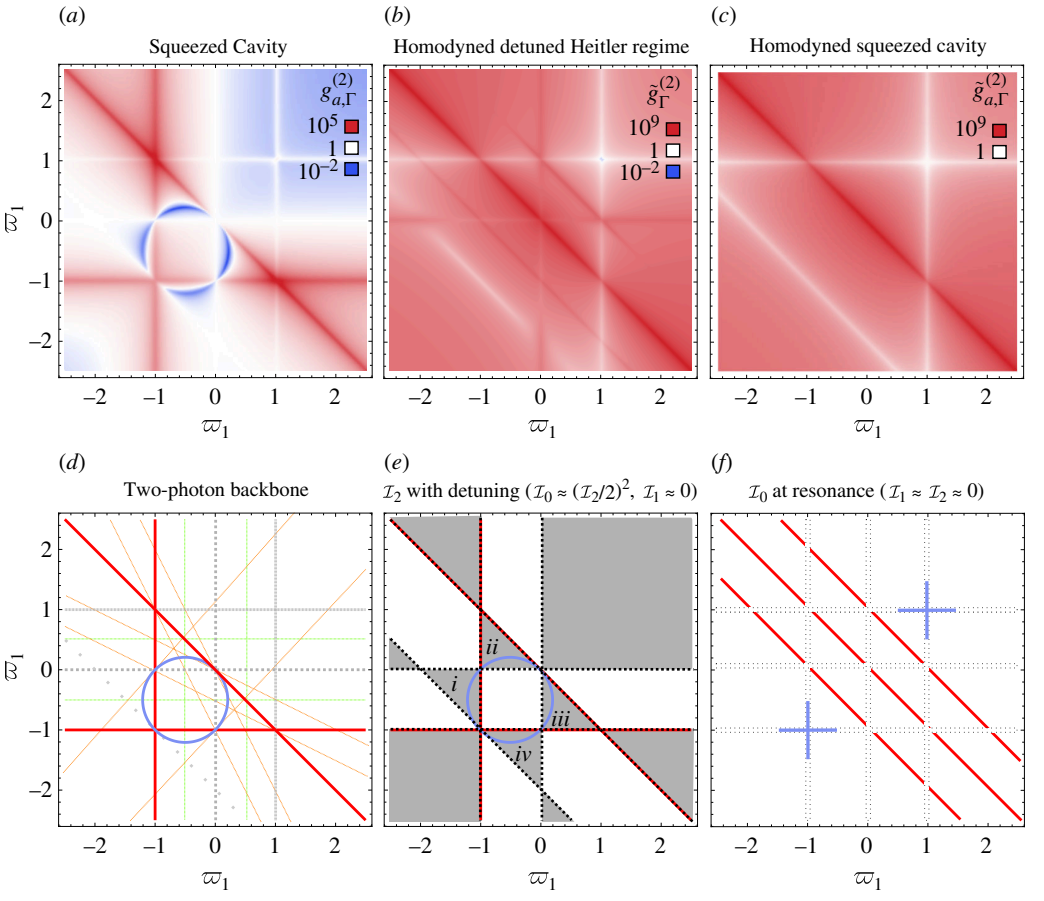

Figure 3. Manifestations of the origin of the circles of antibunching: (*a*) the numerical two-photon spectrum for the squeezed cavity reproduces an almost identical structure to that of exact resonance fluorescence (cf. figure 2*f*). (*b*) The circle is removed when the coherent fraction itself is removed (by homodyning), leaving only the strong superbunching leapfrog processes. This is to be compared with (*c*) the counterpart for the squeezed cavity, which shows that the central antidiagonal also includes a squeezing component. (*d*) The analytical expressions produce an exact circle and straight lines appearing as equation (6.5) and equations (6.6)–(6.7), respectively. The mesh of thin lines are those observed in some two-photon landscapes that go beyond the physics covered in this text. (*e*) and (*f*) show the structure for the main $\mathcal{I}$ coefficients that account for the two-photon spectrum of figure 2, namely, $\mathcal{I}_2$ with detuning and $\mathcal{I}_0$ at resonance. Shaded regions in (*e*) are negative. Parameters: (*a*) $\gamma_a = 1$, $\Delta_a = 80.1$, $\lambda_a = 0.001$ and $\Gamma = 2$, optimizing antibunching. (*b*) is the same as figure 2*f* but with an external homodyning field $\alpha = -\langle\sigma\rangle$.

1*c*,*d* [29]. Our goal now is to show that the one- and two-photon spectra of the coherently squeezed cavity derived in the previous section are, beyond their qualitative agreement with the two-level system, in fact in quantitative agreement to leading order in the driving. This will confirm that in this detuned Heitler regime, and at the two-photon level, the main role of the two-level system is to bring in a component of squeezing, and that the observed phenomenology then follows from two-mode interferences between squeezed and coherent states, with frequencies spanning over all possible modes of the system. The one-photon detuned Heitler spectrum $S_\Gamma(\omega)$ from equation (2.4), with $\Delta_\sigma \gg \Omega_\sigma$, indeed recovers the squeezed-coherent cavity spectrum (equation 5.7) with the correspondence $(\Omega_\sigma^2/\Delta_\sigma^2) \to \Lambda_a/(2\,|\,\Delta_a\,|\,)$. Besides, those are the populations $\langle\sigma^\dagger\sigma\rangle$ and $\langle a^\dagger a\rangle$, respectively. The same occurs with two-photon correlations, although the general expression being awkward, it is not practical to display

here their mathematical identity, which we have, however, checked. We can, instead, highlight particular cases of interest, including the insightful tampering of the photon interferences by filtering out the central peak with a notch filter [59]. In this case, instead of filtering part of the spectrum and correlating it, one filters out another part and correlates what remains. Such an observable could be derived using the frequency-filtered approach described previously, but filtering out the coherent peak is more expediently achieved by homodyning it out, admixing the total luminescence with a laser of matching amplitude α but with opposite phase. If we parameterize this field as $\alpha = -\mathcal{F}\langle\sigma\rangle$ in terms of $0 \leq \mathcal{F} \leq 1$, the two-photon correlations for the homodyned field are found in two limiting cases of interest as:

$$\lim_{\frac{\Delta_\sigma}{\Omega_\sigma}\to\infty} g^{(2)}_{\mathcal{F}}(\tau) = 1 + \frac{1}{(1-\mathcal{F})^4}e^{-\gamma_\sigma\tau} - \frac{2}{(1-\mathcal{F})^2}e^{-(\gamma_\sigma/2)\tau}\cos(\Delta_\sigma\tau)\,, \tag{6.1a}$$

$$\lim_{\mathcal{F}\to 1} g^{(2)}_{\mathcal{F}}(\tau) = 1 + \frac{\Delta_\sigma^4}{4\Omega_\sigma^4}e^{-\gamma_\sigma\tau}\,, \tag{6.1b}$$

where equation (6.1*a*) goes first to the detuned Heitler regime (large detuning and weak driving, the result being independent of how this limit is taken) while equation (6.1*b*) first homodynes the field completely ($\mathcal{F} = 1$, with the coherent peak completely removed so only the incoherent emission is taken). Note that the order of the limits matters, since

$$\lim_{\mathcal{F}\to 1}\lim_{\frac{\Delta_\sigma}{\Omega_\sigma}\to\infty} g^{(2)}_{\mathcal{F}}(\tau) \neq \lim_{\frac{\Delta_\sigma}{\Omega_\sigma}\to\infty}\lim_{\mathcal{F}\to 1} g^{(2)}_{\mathcal{F}}(\tau)\,, \tag{6.2}$$

producing the aforementioned divergencies to leading order. In the first case, only the detuning survives the limit, producing more or less densely populated oscillations between two envelopes depending on whether Δ_σ goes to infinity faster than Ω_σ goes to zero. When $\mathcal{F} = 0$ (no correction, so the full emission is taken, including the laser's scattered light), equation (5.8) is recovered. In the second case, the envelopes have collapsed onto each other so that oscillations are removed and a smooth bunching is observed. These are the two photons ω_υ and ω_σ of figure 1*d* arriving together [59]. The presence of the laser thus allows them to arrive at different times so that their coincidence gets suppressed. This is the origin of antibunching in this case [55]. Oscillations can also be understood as beating due to detuning. More general spectral filtering brings us directly to the full two-photon spectrum. With homodyning, the two-photon spectrum is that of the incoherent part alone and its landscape of correlations transforms from figure 2*f* to figure 3*b*, i.e. the circle disappears. This is another proof of its origin from interferences between the squeezing—that remains and produces extreme bunching (cf. the scale)—and coherence. The result is similar for the squeezed cavity, i.e. with $\Omega_a = 0$, but without the side leapfrogs, the central cross and the antibuching around the real peak, as shown in figure 3*c*. The general two-photon spectrum can be obtained analytically (for both the two-level system and the squeezed cavity, both at and out-of resonance, with or without homodyning), but it is too voluminous to be replicated here. Excellent approximations can, however, be derived in the the highly detuned regime $\Delta_\sigma \gg \Omega_\sigma \gg \gamma_\sigma$, where emission drops due to the inefficient excitation of the system and thus enters in the Heitler regime, although the driving is taken much larger than the decay. As a consequence, the main contribution for the emitted light is the coherent one. To leading order, the population of each sensor $\langle\varsigma_i^\dagger\varsigma_i\rangle$—that both provide, from the sensor method, the spectral shape $S_\Gamma(\varpi)$—recovers the spectral shape equation (5.7), featuring a diverging contribution at the origin that corresponds to the coherent δ peak, in addition to the symmetric side peaks, which are also revealed as not Lorentzian:

$$S_\Gamma(\varpi) = \frac{\epsilon^2\Omega_\sigma^2}{\Delta_\sigma^4}\frac{1}{\varpi^2} + \frac{2\epsilon^2\Omega_\sigma^4}{\Gamma\Delta_\sigma^6}\frac{\Gamma + 2\gamma_\sigma + \Gamma\varpi^2}{(1-\varpi^2)^2} + \text{higher orders}\,. \tag{6.3}$$

The two-photon correlation spectrum is similarly obtained in both cases as:

$$g_{\Gamma}^{(2)}(\varpi_1, \varpi_2) = \frac{(\varpi_1^2 + \varpi_1 + \varpi_2^2 + \varpi_2)^2}{(\varpi_1 + \varpi_2)^2(\varpi_1 + 1)^2(\varpi_2 + 1)^2} + \text{higher orders}. \tag{6.4}$$

This surprisingly compact expression gives an excellent qualitative account of the detuned resonance fluorescence landscape shown in figure 2*f* with divergences and exact zeros that capture the resonances, which get tamed by the higher order corrections as is the case for populations with equation (6.3). From the analysis of the zeros of both the numerator and denominator of this expression, we can thus locate the main features of the two-photon spectrum. Minima correspond to antibunching. They are found by setting the numerator of equation (6.4) to zero, which, rewriting the equation as

$$\left(\varpi_1 + \frac{1}{2}\right)^2 + \left(\varpi_2 + \frac{1}{2}\right)^2 = \frac{1}{2} \tag{6.5}$$

is that of a circle centred at $\varpi_1 = \varpi_2 = -1/2$ and with radius $\sqrt{2}/2$. This not only gives the most compelling explanation for the circle of antibunching—as a two-mode interference between squeezing and coherence—it also shows that it is, indeed, an exact circle. Bunching maxima are actually divergences to leading order and located at the condition that vanish the denominator,

$$\varpi_1 = -1\,, \quad \varpi_2 = -1 \quad \text{and} \quad \varpi_1 + \varpi_2 = 0 \tag{6.6}$$

producing the three main bunching lines of detuned resonance fluorescence, which make a right-angled triangle. Additional maxima can be found looking for the zeros of higher orders (less pronounced in the plot). These are at

$$\varpi_1 = 1\,, \quad \varpi_2 = 1 \quad \text{and} \quad \varpi_1 + \varpi_2 = \pm 1\,. \tag{6.7}$$

The horizontal and vertical correlations now concern the real peak, which is much less correlated than its virtual counterpart. The anti-diagonal lines are the other leapfrog processes. All these lines, along with the circle, are plotted in figure 3*d* as a backbone for the two-photon correlation spectrum. The decomposition of the 2PS into its interference terms, using equation (4.17), leads to:

$$\mathcal{I}_0 \approx \frac{\varpi_1^2\varpi_2^2(2 + \varpi_1 + \varpi_2)^2}{(\varpi_1 + \varpi_2)^2(\varpi_1 + 1)^2(\varpi_2 + 1)^2}\,, \tag{6.8a}$$

$$\mathcal{I}_1 \approx 0, \tag{6.8b}$$

$$\mathcal{I}_2 \approx -\frac{2\varpi_1\varpi_2(2 + \varpi_1 + \varpi_2)}{(\varpi_1 + \varpi_2)(\varpi_1 + 1)(\varpi_2 + 1)}\,. \tag{6.8c}$$

This reveals that, furthermore

$$\mathcal{I}_0 = (\mathcal{I}_2/2)^2 \tag{6.9}$$

which, from equation (4.14), provides $g^{(2)}$ as a function of the squeezing component alone:

$$g_{\Gamma}^{(2)} = \left(1 + \frac{\mathcal{I}_2}{2}\right)^2\,. \tag{6.10}$$

This relationship holds when the coherent fraction dominates over the incoherent, or quantum, fraction, with also phase-matching between them, in which case, squeezing can be related to photon fluctuations [17,38]. This is the case for instance in equation (4.18) when $\phi_1 + \phi_2 - \vartheta_{12} = 0$ or π. This is also the case in the Heitler regime where the coherent fraction overtakes the signal [16,31], including in the presence of filtering [55]. This relationship is the chief reason why squeezing has been more difficult to observe than antibunching [81]. In more general situations,

in particular when $\mathcal{I}_1$ is non-zero, there are deviations from this ideal. The exact numerical results of $\mathcal{I}_i$ for resonance fluorescence are shown in figure 2(*g–o*). The rightmost column of the detuned Heitler regime is well approximated by equations (6.8) with, in particular, $\mathcal{I}_1 \approx 0$ (the darker area means a negative sign for the plotted quantity) and $\mathcal{I}_0$ and $\mathcal{I}_2$ having the redundant appearance from equation 6.9. The squeezing component changes sign on its various domains, as shown in the figure and sketched in figure 3*e* where dark areas indicate negative values. The condition that produces the circle of exact antibunching leads to

$$\mathcal{I}_0 \approx 1, \quad \mathcal{I}_1 \approx 0, \quad \mathcal{I}_2 \approx -2, \tag{6.11}$$

which are the same as those for two-photon suppression from destructive interferences between the squeezing and coherent component of a single mode, but here occurring at the two-photon (with two different frequencies) level. Since $\mathcal{I}_2 < 0$ for this to occur, this happens in the four triangles *i–iv* that corner the circle, as shown in figure 3*e*. The right-angled triangle of bunching defined by the red lines shown in figure 3*e* is also interesting. These lines lie at the frontier of $\mathcal{I}_2$ changing sign, as can be seen in figure 2*o* where they match the dotted lines where $\mathcal{I}_2 = 0$, although it is large (in absolute value) on both sides. The antidiagonal line matches with the central leapfrog line at resonance, which smoothly transforms into the central squeezing line best seen in figure 3*c*. A leapfrog component is retained, however, since the two side leapfrog lines remain visible and only from $\mathcal{I}_0$, as seen in figure 2*i*. The two new lines that appear, horizontal and vertical, betray the virtual character of the peak, which remains correlated, at this pinned frequency, with all the other photons at all the frequencies (this is the novelty as compared with the leapfrog photons). This includes the real photon from the other peak, in which case one realizes the heralded two-photon scheme [68,82,83]. It is noteworthy that not only the circle, but also these vertical and horizontal lines disappear with homodyning (cf. figure 3*b,c*), which shows that they arise from a purely interference effect, but this time a constructive as opposed to destructive one, i.e. corresponding to unconventional (two-mode) bunching according to the terminology of [16]. Interestingly, the anomalous correlator $\mathcal{I}_1$ appears to play a role in the constitution of these 'anomalous' lines, which therefore demand further attention, that is beyond the scope of our current discussion. In contrast, in the first column of figure 2, i.e. at resonance, one has the opposite situation where $\mathcal{I}_0 \gg \mathcal{I}_2$ and, furthermore, $\mathcal{I}_0 < 0$ in the two diagonal quadrants, which contain the spectral peaks (with a meticulous exclusion of the leapfrogs). This signals the non-Gaussian, i.e. Fock, or multi-photon emission, character of both the leapfrogs which have no squeezing associated to their constitution, and of the side peaks, which have the characteristic $\mathcal{I}_0$ of antibunching dominated by the fluctuations of the incoherent emission. The main structure in this case is sketched in figure 3*f* as the two-photon Mollow triplet of leapfrog photons, broken by real transitions. The plus sign (or butterfly) shape of antibunching (in blue) is characteristic of frequency-resolved spontaneous single-photon emission [62] and shows that the side peaks inherit the single-photon character from the two-level system, unlike the central peak due to which path interferences [68]. The second column, as the system transits from one case to the other, shows the 'evaporation' of the negative domain in $\mathcal{I}_0$, which reduces to a tiny islet around the real peak only at high detuning, as well as the emergence and shaping of squeezing in $\mathcal{I}_2$. It also shows the role of the anomalous correlator $\mathcal{I}_1$ in bridging between these two cases, being close to negligible in the other limits.

This achieves our description of the two-photon landscape of resonance fluorescence. All the features have been explained. There is a rich combination of various mechanisms, from multi-photon emission to multi-photon interferences, being realized in different regions of phase space where they can be isolated and exploited. We have largely focused on zero

time-delay, but one could similarly consider the time dynamics of this physics, as we did in [83] where, cross-correlating the side peaks of detuned resonance fluorescence with or without homodyning the coherent peak, we observed a considerable transformation and enhancement of the correlation functions. Clearly, the problem is far from being exhausted. Also, it should be clarified that although at the two-photon level, the physics is captured by two-mode squeezing, the broader problem includes higher photon numbers and goes much beyond this vantage point. One should not make the same mistake with two-photon spectra as has been made with single-photon ones, i.e. assuming that the picture is now complete. This might be the case for the squeezed cavity, since it only involves Gaussian states and thus is fully described through its two-photon correlators, higher-order ones being functions of those. But the two-level system gives rise to non-Gaussian states, and so, the three-photon spectrum (and others of higher orders) are most certainly providing as radical changes as compared with the two-photon case than the two-photon case does to the single-photon one. Some of this higher order physics does in fact indeed transpire in two-photon observables. In the next section, we give a brief overview of a few alternative quantifiers of two-photon emission. There, one will get a chance to sight unaccounted-for phenomena.

7. Violation of inequalities

The above results invite one to seek new regimes of strongly correlated quantum emission, away from the spectral peaks. There is much to prospect for, and various regions (photons of different frequencies) provide us with different types of light. To highlight this point, we compute various quantifiers of non-classical correlations, which can be applied to frequency-filtered photons [84]. We consider here the case of highly detuned resonance fluorescence, since it was not previously considered in this context, and for being both a clean and fruitful source of correlations. We also add a new quantifier for two-mode squeezing, due to the emphasis we have given to its role, also clarifying that while we have compellingly established the importance of squeezing in the broad phenomenology, we are far from having exhausted the topic. Figure 4*a* shows the violation of Cauchy–Schwarz inequalities when $R > 1$ where

$$R \equiv \left[g_{12}^{(2)}\right]^2 / \left[g_{11}^{(2)} g_{22}^{(2)}\right], \tag{7.1}$$

while figure 4*b* shows the violation of Bell's inequalities when $B > 2$ where, this time:

$$B \equiv \sqrt{2}\left|\frac{\langle \varsigma_1^{\dagger 2}\varsigma_1^2\rangle + \langle \varsigma_2^{\dagger 2}\varsigma_2^2\rangle - 4\langle \varsigma_1^\dagger \varsigma_2^\dagger \varsigma_2 \varsigma_1\rangle - \langle \varsigma_1^{\dagger 2}\varsigma_2^2\rangle - \langle \varsigma_2^{\dagger 2}\varsigma_1^2\rangle}{\langle \varsigma_1^{\dagger 2}\varsigma_1^2\rangle + \langle \varsigma_2^{\dagger 2}\varsigma_2^2\rangle + 2\langle \varsigma_1^\dagger \varsigma_2^\dagger \varsigma_2 \varsigma_1\rangle}\right|. \tag{7.2}$$

Figure 4*c* shows two-mode squeezing, which is present if and only if $S > 1$, where [85]:

$$S \equiv \frac{|\langle \varsigma_1^2 \varsigma_2^2\rangle - \langle \varsigma_1 \varsigma_2\rangle^2|}{\langle \varsigma_1^\dagger \varsigma_2^\dagger \varsigma_2 \varsigma_1\rangle - |\langle \varsigma_1\rangle\langle \varsigma_2\rangle|^2}. \tag{7.3}$$

From the Cauchy–Schwarz inequality, one can see again in figure 4 the region of no-coincidence emission, where the system stops emitting at the two-photon level, which is the black circle. This quantity might be even more suitable to identify the region of no two-photon emission, being a more properly normalized version of two-photon correlations. It generalizes spectral line elimination via quantum interferences in spontaneous emission [86] to the case of two-photon emission. The green regions show non-classical emission. Since the main diagonal is white, it means that the emission at any frequency from the spectrum is classical, which is also the case at resonance [84]. Both the main leapfrog and photons involving the virtual peak are strongly quantum correlated, and are likely valuable resources for quantum emitters of a new type. The Bell inequality is, interestingly, of a quite different character, being mainly attached to the main leapfrog (as well as a little to the circle of no two-photon emission, surprisingly) where,

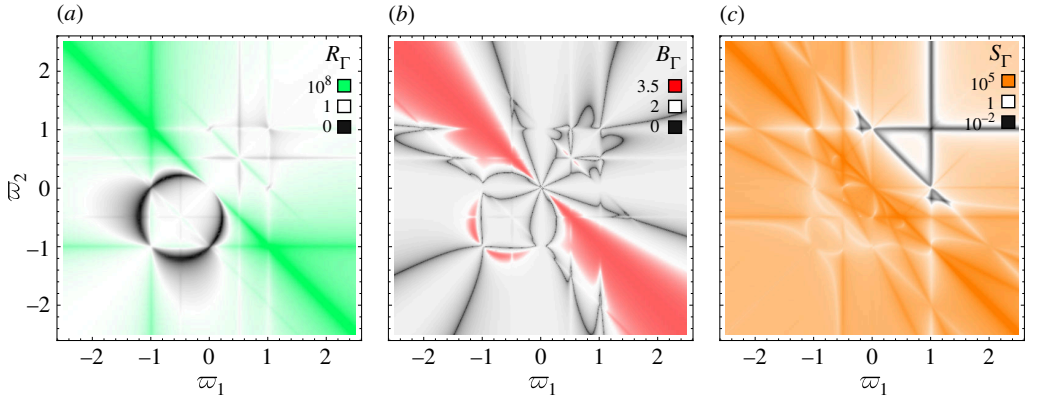

Figure 4. Violations of (*a*) Cauchy and (*b*) Bell inequalities in highly detuned resonance fluorescence, as well as presence of (*c*) two-mode squeezing. Filtering harvests correlations. Sight of new physics beyond that discussed in the text is also apparent. Parameters are the same as for figure 2*f*.

unlike other quantifiers that behave more like resonances, it spreads and increases as one gets away from the triplet. Those are features that we cannot currently explain. Finally, figure 4*c*, which indicates two-mode squeezing, is probably the most interesting as it first confirms that this is a feature to be found almost everywhere in detuned resonance fluorescence, except in the vicinity of the real peaks. More interestingly, however, new lines whose slope betray other photon combinations ($2\varpi_1 + \varpi_2 = k$ and $\varpi_1 + 2\varpi_2 = k$ where $k = -1$ or 0) reveal that there is rich additional physics that we have not yet touched upon, possibly involving squeezed correlations of higher photon numbers. Even at the qualitative level of explaining the basic but strong features that shape the landscape, we find evidence of more complicated processes inherited from beyond two-photon physics. Some of them have been discussed through $g^{(n)}$ correlators at resonance [67]. The features not yet accounted for from the quantifiers discussed in this section are reported in figure 3*d* as thin lines, requiring new physics. In its pursuit, we could indeed, using the same approach and techniques, but computing other observables, characterize other types of correlations, such as three-mode squeezing, other types of entanglement, quadrature-based tripartite inseparability [87,88], etc. It is clear that there remains much to explore, understand and turn into devices, even with the simplest problem of quantum optics, while the same approach can be applied to more complicated systems, from cosmic radiation to atoms and molecules passing by condensed matter and other types of quantum emitters.

8. Conclusion and outlook

We have provided a detailed, and essentially analytical, picture of the two-photon physics of resonance fluorescence. Maybe the most important message is that this should be contemplated on its own, independently from one-photon observables, however ingrained is one's attachment to intensity, signal and photoluminescence spectra. This text was written at the invitation of the Royal Society to commemorate the Newton International Fellowship awarded to one of us (EdV, in 2009). It brings together various of EdV's research lines, which started at this occasion with a theory of lasing that produced the Mollow triplet with coherence provided by the emitter itself as opposed to being brought from outside [80]. This led her to study in more details the coupling (and decoupling) of two-level systems [89] and how they develop and maintain correlations in the steady state [90], sustaining a rich span of different regimes interpolating between incoherent and coherent [91], from the interplay of quantum and dissipative light-matter interactions. The need to scrutinize as completely as possible photon

correlations from such platforms led to the introduction of the frequency degree of freedom, this time as part of a Humboldt Fellowship. This provides the first pillar on which stands the edifice that explains the two-photon physics of resonance fluorescence (and a wealth of other problems in its wake): the theory of frequency-resolved multi-photon correlations [15,61]. The other pillar is the theory of quantum field admixtures [16]. Remarkably, while these have been pursued independently, they turn out to be naturally and deeply interconnected, besides, on what is possibly the simplest-possible non-trivial problem of quantum optics: the coherently driven two-level system. We believe that this betrays the extremely fundamental and universal character of these concepts. The other authors of this text, as we are sure would also our past collaborators on these topics, concur that the surprisingly complex and rich phenomenology that is being revealed, far from exhausting or completing the description of the problem, is only making it even more mysterious and unfathomable. This evokes to us the aphorism of Newton himself:

> I seem to have been only like a boy playing on the sea-shore, and diverting myself in now and then finding a smoother pebble or a prettier shell than ordinary, whilst the great ocean of truth lay all undiscovered before me.

While we have for brevity, simplicity and current experimental interest, focused on two-photon physics, the above approach is completely general and can, indeed inevitably will, be generalized to multi-photon correlations and n-mode squeezing. Spheres of antibunching [67] have already been spotted in three-photon correlation spectra and it is obvious that resonance fluorescence abounds with three-mode squeezing that remains to be characterized, measured and exploited. Among other compelling immediate continuations of this work, we can mention (i) seizing additional control and tuneability of the correlations by externally adjusting the interferences with a laser [31], (ii) using strongly correlated two-photon spectral locations for quantum-spectroscopic applications [92], or (iii) Purcell-enhancing them to realize new types of devices with high-purity and strong signal [74]. There are definitely still other and possibly even more exciting prospects. At any rate, it is clear that, although inconspicuous at the one-photon level, there is a rich and varied two-photon physics, which takes place everywhere.

Data accessibility. This article has no additional data.

Declaration of AI use. We have not used AI-assisted technologies in creating this article.

Authors' contributions. E.Z.C.: conceptualization, data curation, formal analysis, investigation, methodology, resources, software, supervision, validation, visualization, writing—original draft, writing—review and editing; F.P.L.: conceptualization, data curation, formal analysis, funding acquisition, investigation, methodology, project administration, resources, software, supervision, validation, visualization, writing—original draft, writing—review and editing; E.dV.: conceptualization, data curation, formal analysis, funding acquisition, investigation, methodology, project administration, resources, supervision, validation, visualization, writing—original draft, writing—review and editing.

All authors gave final approval for publication and agreed to be held accountable for the work performed therein.

Conflict of interest declaration. We declare we have no competing interests.

Funding. E.d.V. acknowledges support from the CAM Pricit Plan (Ayudas de Excelencia del Profesorado Universitario), TUM-IAS Hans Fischer Fellowship and projects AEI/10.13039/501100011033 (2DEnLight) and Sinérgico CAM 2020 Y2020/TCS-6545 (NanoQuCo-CM). F.P.L. acknowledges the HORIZON EIC-2022-PATHFINDERCHALLENGES-01 HEISINGBERG project 101114978. This work was written at the invitation of EdV's Newton Fellowship, which is also gratefully acknowledged.

Acknowledgements. We acknowledge discussions with and interest from colleagues throughout the years, in particular Juan Camilo López Carreño, Carlos Sánchez Muñoz, Alejandro González Tudela, Carlos Antón Solanas, Carlos Tejedor, Sang Kyu Kim and Kai Müller. We dedicate this text to Bruno Doncel Sánchez, who was born on the day this work was submitted.

References

1. Bohr N. 1913 On the constitution of atoms and molecules. *Philos. Mag.* **26**, 1. (doi:10.1080/14786441308634955)
2. Slipher VM. 1912 On the spectrum of the nebula in the Pleiades. *Low. Obs. Bull.* **2**, 26. https://ui.adsabs.harvard.edu/abs/1912LowOB...2...26S/abstract
3. Page TL. 1936 The continuous spectra of certain planetary nebulae: a photometric study. *Mon. Not. R. Astron. Soc.* **96**, 604–635. (doi:10.1093/mnras/96.6.604)
4. Zanstra H. 1936 An argument against scattering in planetary nebulae. *Observatory* **59**, 314. https://ui.adsabs.harvard.edu/abs/1936Obs....59..314Z/abstract
5. Kipper A. 1950 Sbornik ``O Razvitii Sovetskoi Nauki v E'stonckoi S.S.R.'' (on the development of Soviet science in the Estonean S.S.R. *Tallin.* **316**.
6. Spitzer L Jr, Greenstein JL. 1951 Continuous emission from planetary nebulae. *Astrophys. J.* **114**, 407. (doi:10.1086/145480)
7. Göppert Mayer M. 1929 Über die Wahrscheinlichkeit des Zusammenwirkens zweier Lichtquanten in einem Elementarakt. *Naturwissenschaften* **17**, 932–932. (doi:10.1007/BF01506585)
8. Breit G, Teller E. 1940 Metastability of hydrogen and helium levels. *Astrophys. J.* **91**, 215. (doi:10.1086/144158)
9. Lipeles M, Novick R, Tolk N. 1965 Direct detection of two-photon emission from the metastable state of singly ionized helium. *Phys. Rev. Lett.* **15**, 690–693. (doi:10.1103/PhysRevLett.15.690)
10. Zalialiutdinov TA, Solovyev DA, Labzowsky LN, Plunien G. 2018 QED theory of multiphoton transitions in atoms and ions. *Phys. Rep.* **737**, 1–84. (doi:10.1016/j.physrep.2018.02.003)
11. Tung JH, Salamo XM, Chan FT. 1984 Two-photon decay of hydrogenic atoms. *Phys. Rev. A* **30**, 1175–1184. (doi:10.1103/PhysRevA.30.1175)
12. Yatsiv S, Rokni M, Barak S. 1968 Enhanced two-proton emission. *Phys. Rev. Lett.* **20**, 1282–1284. (doi:10.1103/PhysRevLett.20.1282)
13. Hayat A, Ginzburg P, Orenstein M. 2008 Observation of two-photon emission from semiconductors. *Nat. Photon.* **2**, 238–241. (doi:10.1038/nphoton.2008.28)
14. Rivera N, Kaminer I, Zhen B, Joannopoulos JD, Soljačić M. 2016 Shrinking light to allow forbidden transitions on the atomic scale. *Science* **353**, 263–269. (doi:10.1126/science.aaf6308)
15. del Valle E, Gonzalez-Tudela A, Laussy FP, Tejedor C, Hartmann MJ. 2012 Theory of frequency-filtered and time-resolved n-photon correlations. *Phys. Rev. Lett.* **109**, 183601. (doi:10.1103/PhysRevLett.109.183601)
16. Zubizarreta Casalengua E, López Carreño JC, Laussy FP, del Valle E. 2020 Conventional and unconventional photon statistics. *Laser Photon. Rev.* **14**, 1900279. (doi:10.1002/lpor.201900279)
17. Loudon R. 1984 Squeezing in resonance fluorescence. *Opt. Commun.* **49**, 24–28. (doi:10.1016/0030-4018(84)90083-X)
18. Holm DA, Sargent M. 1985 Theory of two-photon resonance fluorescence. *Opt. Lett.* **10**, 405. (doi:10.1364/OL.10.000405)
19. Lewenstein M, Zhu Y, Mossberg TW. 1990 Two-photon gain and lasing in strongly driven two-level atoms. *Phys. Rev. Lett.* **64**, 3131–3134. (doi:10.1103/PhysRevLett.64.3131)
20. Heitler W. 1954 *The quantum theory of radiation*, 3rd edn. London, UK: Oxford University Press.
21. Mollow BR. 1969 Power spectrum of light scattered by two-level systems. *Phys. Rev.* **188**, 1969–1975. (doi:10.1103/PhysRev.188.1969)
22. Eberly JH, Wódkiewicz K. 1977 The time-dependent physical spectrum of light. *J. Opt. Soc. Am.* **67**, 1252. (doi:10.1364/JOSA.67.001252)
23. Gardiner CW. 1993 Driving a quantum system with the output field from another driven quantum system. *Phys. Rev. Lett.* **70**, 2269–2272. (doi:10.1103/PhysRevLett.70.2269)
24. Carmichael HJ. 1993 Quantum trajectory theory for cascaded open systems. *Phys. Rev. Lett.* **70**, 2273–2276. (doi:10.1103/PhysRevLett.70.2273)

25. López Carreño JC, del Valle E, Laussy FP. 2018 Frequency-resolved Monte Carlo. *Sci. Rep.* **8**, 6975. (doi:10.1038/s41598-018-24975-y)
26. del Valle E, Laussy FP. 2013 Mollow triplet. *Wolfram demonstrations project*. See https://demonstrations.wolfram.com/MollowTriplet.
27. Cohen-Tannoudji CN, Reynaud S. 1977 Dressed-atom description of resonance fluorescence and absorption spectra of a multi-level atom in an intense laser beam. *J. Phys. B At. Mol. Phys.* **10**, 345–363. (doi:10.1088/0022-3700/10/3/005)
28. Reynaud S, Dalibard J, Cohen-Tannoudji C. 1988 Photon statistics and quantum jumps: the picture of the dressed atom radiative cascade. *IEEE J. Quantum Electron.* **24**, 1395–1402. (doi:10.1109/3.979)
29. Dalibard J, Reynaud S. 1983 Correlation signals in resonance fluorescence: interpretation via photon scattering amplitudes. *J. Phys. France* **44**, 1337–1343. (doi:10.1051/jphys:0198300440120133700)
30. Cohen-Tannoudji C, Reynaud S. 2016 Dressed-atom description of resonance fluorescence of atoms coupled to intense laser beams. *J. Phys. B At. Mol. Opt. Phys.* **49**, 200502. (doi:10.1088/0953-4075/49/20/200502)
31. López Carreño JC, Zubizarreta Casalengua E, Laussy FP, del Valle E. 2018 Joint subnatural-linewidth and single-photon emission from resonance fluorescence. *Quantum Sci. Technol.* **3**, 045001. (doi:10.1088/2058-9565/aacfbe)
32. Carmichael HJ, Walls DF. 1976 A quantum-mechanical master equation treatment of the dynamical stark effect. *J. Phys. B At. Mol. Phys.* **9**, 1199–1219. (doi:10.1088/0022-3700/9/8/007)
33. Zubizarreta Casalengua E, del Valle E, Laussy FP. 2024 Photon liquefaction in time. *APL Quant.* **1**, 026117. (doi:10.1063/5.0206213)
34. Nguyen HS *et al.* 2011 Ultra-coherent single photon source. *Appl. Phys. Lett.* **99**, 261904. (doi:10.1063/1.4719077)
35. Matthiesen C, Vamivakas AN, Atatüre M. 2012 Subnatural linewidth single photons from a quantum dot. *Phys. Rev. Lett.* **108**, 093602. (doi:10.1103/PhysRevLett.108.093602)
36. Centeno Neelen R, Boersma DM, van Exter MP, Nienhuis G, Woerdman JP. 1992 Spectral filtering within the Schawlow-Townes linewidth of a semiconductor laser. *Phys. Rev. Lett.* **69**, 593–596. (doi:10.1103/PhysRevLett.69.593)
37. Lemonde MA, Didier N, Clerk AA. 2014 Antibunching and unconventional photon blockade with Gaussian squeezed states. *Phys. Rev. A* **90**, 063824. (doi:10.1103/PhysRevA.90.063824)
38. Mandel L. 1982 Squeezed states and sub-Poissonian photon statistics. *Phys. Rev. Lett.* **49**, 136–138. (doi:10.1103/PhysRevLett.49.136)
39. Arnoldus HF, Nienhuis G. 1983 Conditions for sub-Poissonian photon statistics and squeezed states in resonance fluorescence. *Opt. Acta* **30**, 1573–1585. (doi:10.1080/713821098)
40. Stoler D. 1970 Equivalence classes of minimum uncertainty packets. *Phys. Rev. D* **1**, 3217–3219. (doi:10.1103/PhysRevD.1.3217)
41. Glauber R. 1964 Optical coherence and photon statistics. In *Quantum optics and electronics* (eds C DeWitt, A Blandin, C Cohen-Tannoudji). New York: Gordon and Breach.
42. Walls DF, Zoller P. 1981 Reduced quantum fluctuations in resonance fluorescence. *Phys. Rev. Lett.* **47**, 709–711. (doi:10.1103/PhysRevLett.47.709)
43. Kimble HJ, Dagenais M, Mandel L. 1977 Photon antibunching in resonance fluorescence. *Phys. Rev. Lett.* **39**, 691–695. (doi:10.1103/PhysRevLett.39.691)
44. Lu ZH, Bali S, Thomas JE. 1998 Observation of squeezing in the phase-dependent fluorescence spectra of two-level atoms. *Phys. Rev. Lett.* **81**, 3635–3638. (doi:10.1103/PhysRevLett.81.3635)
45. Carmichael HJ. 1985 Photon antibunching and squeezing for a single atom in a resonant cavity. *Phys. Rev. Lett.* **55**, 2790–2793. (doi:10.1103/PhysRevLett.55.2790)
46. Ou ZYJ. 2007 *Multi-photon quantum interference*. New York, NY: Springer.
47. Ficek Z, Swain S. 2004 *Quantum interference and coherence: theory and experiments*. Springer.
48. Zubizarreta Casalengua E, López Carreño JC, Laussy FP, del Valle E. 2020 Tuning photon statistics with coherent fields. *Phys. Rev. A* **101**, 063824. (doi:10.1103/PhysRevA.101.063824)
49. Loudon R. 2000 *The quantum theory of light*, 3rd edn. Oxford Science Publications.

50. Carmichael HJ. 2002 *Statistical methods in quantum optics 1*, 2nd edn. Berlin Heidelberg, Germany: Springer Verlag.
51. Stoler D. 1974 Photon antibunching and possible ways to observe it. *Phys. Rev. Lett.* **33**, 1397–1400. (doi:10.1103/PhysRevLett.33.1397)
52. Kimble HJ, Mandel L. 1976 Theory of resonance fluorescence. *Phys. Rev. A***13**, 2123–2144. (doi:10.1103/PhysRevA.13.2123)
53. Koashi M, Kono K, Hirano T, Matsuoka M. 1993 Photon antibunching in pulsed squeezed light generated via parametric amplification. *Phys. Rev. Lett.* **71**, 1164–1167. (doi:10.1103/PhysRevLett.71.1164)
54. Lu YJ, Ou ZY. 2002 Observation of nonclassical photon statistics due to quantum interference. *Phys. Rev. Lett.* **88**, 023601. (doi:10.1103/PhysRevLett.88.023601)
55. Hanschke L *et al.* 2020 Origin of antibunching in resonance fluorescence. *Phys. Rev. Lett.* **125**, 170402. (doi:10.1103/PhysRevLett.125.170402)
56. López Carreño JC, Zubizarreta Casalengua E, Silva B, del Valle E, Laussy FP. 2022 Loss of antibunching. *Phys. Rev. A* **105**, 023724. (doi:10.1103/PhysRevA.105.023724)
57. Fischer KA, Müller K, Rundquist A, Sarmiento T, Piggott AY, Kelaita Y, Dory C, Lagoudakis KG, Vučković J. 2016 Self-homodyne measurement of a dynamic Mollow triplet in the solid state. *Nat. Photonics* **10**, 163–166. (doi:10.1038/nphoton.2015.276)
58. Phillips CL, Brash AJ, McCutcheon DPS, Iles-Smith J, Clarke E, Royall B, Skolnick MS, Fox AM, Nazir A. 2020 Photon statistics of filtered resonance fluorescence. *Phys. Rev. Lett.* **125**, 043603. (doi:10.1103/PhysRevLett.125.043603)
59. Masters L, Hu XX, Cordier M, Maron G, Pache L, Rauschenbeutel A, Schemmer M, Volz J. 2023 On the simultaneous scattering of two photons by a single two-level atom. *Nat. Photonics* **17**, 972–976. (doi:10.1038/s41566-023-01260-7)
60. Glauber RJ. 1963 Photon correlations. *Phys. Rev. Lett.* **10**, 84–86. (doi:10.1103/PhysRevLett.10.84)
61. del Valle E. 2013 Distilling one, two and entangled pairs of photons from a quantum dot with cavity QED effects and spectral filtering. *New J. Phys.* **15**, 025019. (doi:10.1088/1367-2630/15/2/025019)
62. González-Tudela A, Laussy FP, Tejedor C, Hartmann MJ, del Valle E. 2013 Two-photon spectra of quantum emitters. *New J. Phys.* **15**, 033036. (doi:10.1088/1367-2630/15/3/033036)
63. Arnoldus HF, Nienhuis G. 1984 Photon correlations between the lines in the spectrum of resonance fluorescence. *J. Phys. B At. Mol. Phys.* **17**, 963–977. (doi:10.1088/0022-3700/17/6/011)
64. Knoll L, Weber G. 1986 Theory of n-fold time-resolved correlation spectroscopy and its application to resonance fluorescence radiation. *J. Phys. B At. Mol. Phys.* **19**, 2817–2824. (doi:10.1088/0022-3700/19/18/012)
65. Cresser JD. 1987 Intensity correlations of frequency-filtered light fields. *J. Phys. B At. Mol. Phys.* **20**, 4915–4927. (doi:10.1088/0022-3700/20/18/027)
66. González-Tudela A, del Valle E, Laussy FP. 2015 Optimization of photon correlations by frequency filtering. *Phys. Rev. A* **91**, 043807. (doi:10.1103/PhysRevA.91.043807)
67. López Carreño JC, del Valle E, Laussy FP. 2017 Photon correlations from the Mollow triplet. *Laser Photon. Rev.* **11**, 1700090. (doi:10.1002/lpor.201700090)
68. Schrama CA, Nienhuis G, Dijkerman HA, Steijsiger C, Heideman HGM. 1992 Intensity correlations between the components of the resonance fluorescence triplet. *Phys. Rev. A* **45**, 8045–8055. (doi:10.1103/physreva.45.8045)
69. Nienhuis G. 1993 Spectral correlations in resonance fluorescence. *Phys. Rev. A* **47**, 510–518. (doi:10.1103/physreva.47.510)
70. Peiris M, Petrak B, Konthasinghe K, Yu Y, Niu ZC, Muller A. 2015 Two-color photon correlations of the light scattered by a quantum dot. *Phys. Rev. B* **91**, 195125. (doi:10.1103/PhysRevB.91.195125)
71. Peiris M, Konthasinghe K, Muller A. 2017 Franson interference generated by a two-level system. *Phys. Rev. Lett.* **118**, 030501. (doi:10.1103/PhysRevLett.118.030501)
72. Nieves Y, Muller A. 2018 Third-order frequency-resolved photon correlations in resonance fluorescence. *Phys. Rev. B* **98**, 165432. (doi:10.1103/PhysRevB.98.165432)
73. Nieves Y, Muller A. 2020 Third-order photon cross-correlations in resonance fluorescence. *Phys. Rev. B* **102**, 155418. (doi:10.1103/PhysRevB.102.155418)

74. Sánchez Muñoz C, del Valle E, Gonzalez-Tudela A, Müller K, Lichtmannecker S, Kaniber M, Tejedor C, Finley JJ, Laussy FP. 2014 Emitters of N-photon bundles. *Nat. Photonics* **8**, 550–555. (doi:10.1038/nphoton.2014.114)
75. Walls DF. 1983 Squeezed states of light. *Nature* **306**, 141–146. (doi:10.1038/306141a0)
76. Caves CM. 1981 Quantum-mechanical noise in an interferometer. *Phys. Rev. D* **23**, 1693–1708. (doi:10.1103/PhysRevD.23.1693)
77. Yuen HP. 1976 Two-photon coherent states of the radiation field. *Phys. Rev. A* **13**, 2226–2243. (doi:10.1103/PhysRevA.13.2226)
78. Ma X, Rhodes W. 1990 Multimode squeeze operators and squeezed states. *Phys. Rev. A* **41**, 4625–4631. (doi:10.1103/physreva.41.4625)
79. Georgiades NP, Polzik ES, Kimble HJ. 1999 Quantum interference in two-photon excitation with squeezed and coherent fields. *Phys. Rev. A***59**, 676–690. (doi:10.1103/PhysRevA.59.676)
80. del Valle E, Laussy FP. 2010 Mollow triplet under incoherent pumping. *Phys. Rev. Lett.* **105**, 233601. (doi:10.1103/PhysRevLett.105.233601)
81. Schulte CHH, Hansom J, Jones AE, Matthiesen C, Le Gall C, Atatüre M. 2015 Quadrature squeezed photons from a two-level system. *Nature* **525**, 222–225. (doi:10.1038/nature14868)
82. Ulhaq A, Weiler S, Ulrich SM, Roßbach R, Jetter M, Michler P. 2012 Cascaded single-photon emission from the Mollow triplet sidebands of a quantum dot. *Nat. Photonics* **6**, 238–242. (doi:10.1038/nphoton.2012.23)
83. Zubizarreta Casalengua E, del Valle E, Laussy FP. 2023 Two-photon correlations in detuned resonance fluorescence. *Phys. Scr.* **98**, 055104. (doi:10.1088/1402-4896/acc89e)
84. Sánchez Muñoz C, del Valle E, Tejedor C, Laussy FP. 2014 Violation of classical inequalities by photon frequency filtering. *Phys. Rev. A* **90**, 052111. (doi:10.1103/PhysRevA.90.052111)
85. Hillery M. 1989 Sum and difference squeezing of the electromagnetic field. *Phys. Rev. A* **40**, 3147–3155. (doi:10.1103/PhysRevA.40.3147)
86. Zhu S, Scully MO. 1996 Spectral line elimination and spontaneous emission cancellation via quantum interference. *Phys. Rev. Lett.* **76**, 388–391. (doi:10.1103/PhysRevLett.76.388)
87. Armstrong S, Wang M, Teh RY, Gong Q, He Q, Janousek J, Bachor HA, Reid MD, Lam PK. 2015 Multipartite Einstein–Podolsky–Rosen steering and genuine tripartite entanglement with optical networks. *Nat. Phys.* **11**, 167–172. (doi:10.1038/nphys3202)
88. Shalm LK, Hamel DR, Yan Z, Simon C, Resch KJ, Jennewein T. 2013 Three-photon energy–time entanglement. *Nat. Phys.* **9**, 19–22. (doi:10.1038/nphys2492)
89. del Valle E. 2010 Strong and weak coupling of two coupled qubits. *Phys. Rev. A* **81**, 053811. (doi:10.1103/PhysRevA.81.053811)
90. del Valle E. 2011 Steady-state entanglement of two coupled qubits. *J. Opt. Soc. Am. B* **28**, 228. (doi:10.1364/JOSAB.28.000228)
91. del Valle E, Laussy FP. 2011 Regimes of strong light-matter coupling under incoherent excitation. *Phys. Rev. A* **84**, 043816. (doi:10.1103/PhysRevA.84.043816)
92. Mukamel S *et al.* 2020 Roadmap on quantum light spectroscopy. *J. Phys. B* **53**, 072002. (doi:10.1088/1361-6455/ab69a8)